

Improved Asymptotic Formulae for Statistical Interpretation Based on Likelihood Ratio Tests

Li-Gang Xia^a, Yan Zhang

School of Physics, Nanjing University

No. 22 Hankou Road, Nanjing, China

Abstract

In this work, we try to improve the classic asymptotic formulae to describe the probability distribution of likelihood-ratio statistical tests. The idea is to split the probability distribution function into two parts. One part is universal and described by the asymptotic formulae. The other part is case-dependent and estimated explicitly using a 6-bin model proposed in this work. The latter is similar to doing toy simulations and hence is able to predict the discrete structures in the probability distributions. The new asymptotic formulae provide a much better differential description of the test statistics. The better performance is confirmed in two toy examples.

arXiv:2101.06944v7 [physics.data-an] 15 Feb 2024

^a ligang.xia@cern.ch

I. INTRODUCTION

Searching for new physics is always the goal for most experimenters in particle physics, especially after the discovery of the Higgs boson [1, 2]. Once a measurement is done, it is important to report the results in a precise and well-accepted way. One often reports two things if no significant signal is observed. One is the probability that the observation is due to the fluctuation of known backgrounds. This is used to represent the statistical significance of a signal and to establish its discovery. The other is the parameter space about the new signal that the measurement can exclude for a given confidence level (C.L.). To interpret the results, we usually build a test statistic based on the likelihood ratio, which is the most powerful discriminant. To find the statistical significance and the exclusion limits, we need to know the probability distribution of the statistical test under many hypotheses with different signal strengths or other parameter of interest (POI). We can resort to toy Monte Carlo (MC) simulation. But it is usually computationally expensive.

Fortunately, asymptotic formulae have been found in Ref. [3] to describe the distribution of the likelihood ratio tests if the sample size is big enough. Therefore, one can easily obtain the expected statistical significance and exclusion limits for a new signal based on the idea of “asimov” dataset [3]. The validity of the asymptotic formulae is based on a theorem by Wald [4] and the condition is that the sample size is sufficiently big. Recently, one of the authors has finished a study of the feasibility to search for leptoquarks in Pb-Pb ultra-peripheral collisions [5] and the background level in that case is very low (the expected number of background events is much less than 1). It is the direct motivation of the current work to improve the asymptotic formulae.

In Sec. II, we will have a brief review about the test statistic and the classic asymptotic formulae. In Sec. III, we will elaborate two improvements and present the new formulae. The two sets of asymptotic formulae are compared using two examples in Sec. IV. Sec. V is a short summary.

TABLE I. Summary of the test statistics based on the likelihood ratio

Test statistic	Purpose
t_0	to establish the discovery of a signal
t_μ	to set a confidence interval of a signal at a given level
q_μ	to set an upper limit of a signal at a given level
q_0	to establish the discovery of a positive signal
\tilde{t}_μ	to set a confidence interval of a positive signal at a given level
\tilde{q}_μ	to set an upper limit of a positive signal at a given level

II. REVIEW OF THE TEST STATISTIC AND THE ASYMPTOTIC FORMULAE

We will review the test statistics and the asymptotic formulae according to Ref. [3]. To test a hypothesis with the signal strength μ , we consider the likelihood ratio

$$\lambda(\mu) = \frac{\mathcal{L}(\mu, \hat{\boldsymbol{\theta}}(\mu))}{\mathcal{L}(\hat{\mu}, \hat{\boldsymbol{\theta}})}, \quad (1)$$

where $\boldsymbol{\theta}$ denotes a set of nuisance parameters; $\hat{\mu}$ and $\hat{\boldsymbol{\theta}}$ are the optimal values to maximize the likelihood function; $\hat{\boldsymbol{\theta}}(\mu)$ are the optimal values with μ fixed and can be seen as functions of μ . Based on this ratio, six test statistics, namely, $t_0, q_0, t_\mu, \tilde{t}_\mu, q_\mu$ and \tilde{q}_μ , are defined for different purposes. They are summarized in Table I.

To have a feeling, Fig. 1-6 show the distribution of the six test statistics versus the signal strength from the toy MC simulations of Ex. 0, which will be used in Sec. IV. The asymptotic relations predicted by Wald's theorem are also shown.

For example, to set an upper limit on μ , the recommendation is q_μ .

$$\tilde{q}_\mu = \begin{cases} 0 & \hat{\mu} > \mu, \\ -2 \ln \frac{\mathcal{L}(\mu, \hat{\boldsymbol{\theta}}(\mu))}{\mathcal{L}(\hat{\mu}, \hat{\boldsymbol{\theta}})} & \hat{\mu} \leq \mu, \end{cases} \quad (2)$$

If further considering the constraint $\mu > 0$ (assuming that the signal contribution to the observed number of events is positive), the recommendation is \tilde{q}_μ .

$$\tilde{q}_\mu = \begin{cases} 0 & \hat{\mu} > \mu, \\ -2 \ln \frac{\mathcal{L}(\mu, \hat{\boldsymbol{\theta}}(\mu))}{\mathcal{L}(\hat{\mu}, \hat{\boldsymbol{\theta}})} & \mu \geq \hat{\mu} \geq 0, \\ -2 \ln \frac{\mathcal{L}(\mu, \hat{\boldsymbol{\theta}}(\mu))}{\mathcal{L}(0, \hat{\boldsymbol{\theta}}(0))} & \hat{\mu} < 0. \end{cases} \quad (3)$$

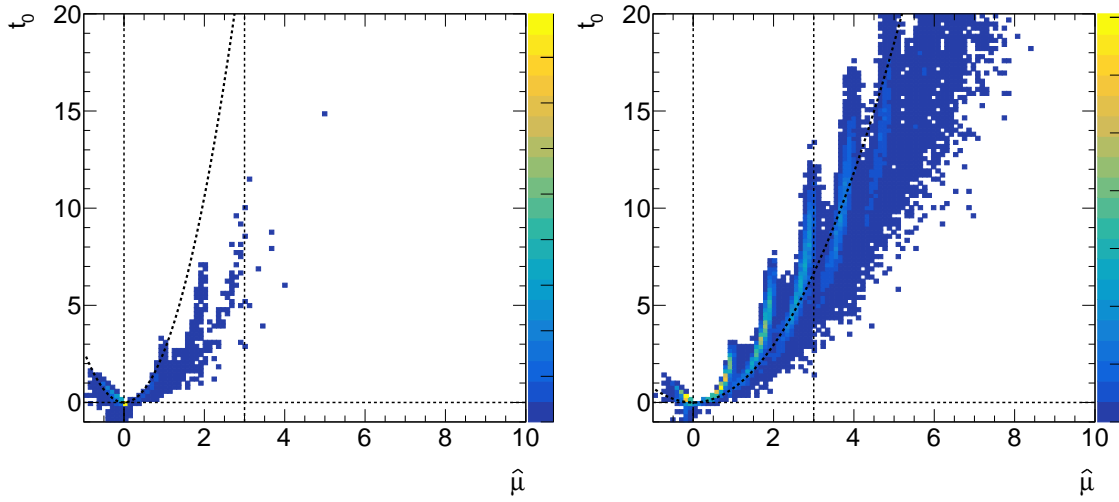


FIG. 1. The distribution of $t_0 : \hat{\mu}$ in Ex. 0 of Sec. IV for the hypothesized signal strength $\mu_H = 0$ (L) and $\mu_H = 3$ (R). The bold dashed curves represent the asymptotic relation from Wald's theorem.

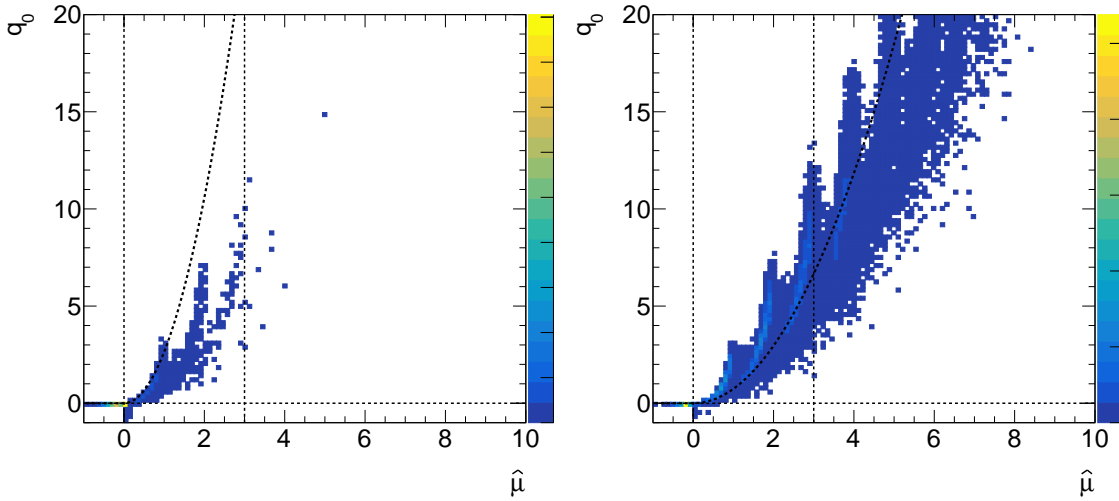


FIG. 2. The distribution of $q_0 : \hat{\mu}$ in Ex. 0 of Sec. IV for the hypothesized signal strength $\mu_H = 0$ (L) and $\mu_H = 3$ (R). The bold dashed curves represent the asymptotic relation from Wald's theorem.

To reject the background-only hypothesis (namely, $\mu = 0$), the recommended test statistic

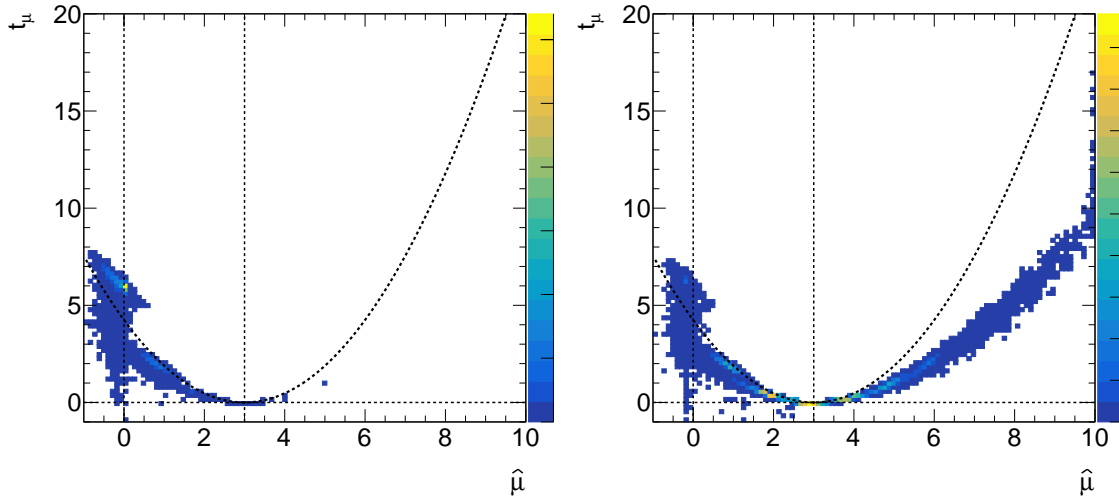


FIG. 3. The distribution of $t_{\hat{\mu}} : \hat{\mu}$ in Ex. 0 of Sec. IV for the hypothesized signal strength $\mu_H = 0$ (L) and $\mu_H = 3$ (R). The bold dashed curves represent the asymptotic relation from Wald's theorem.

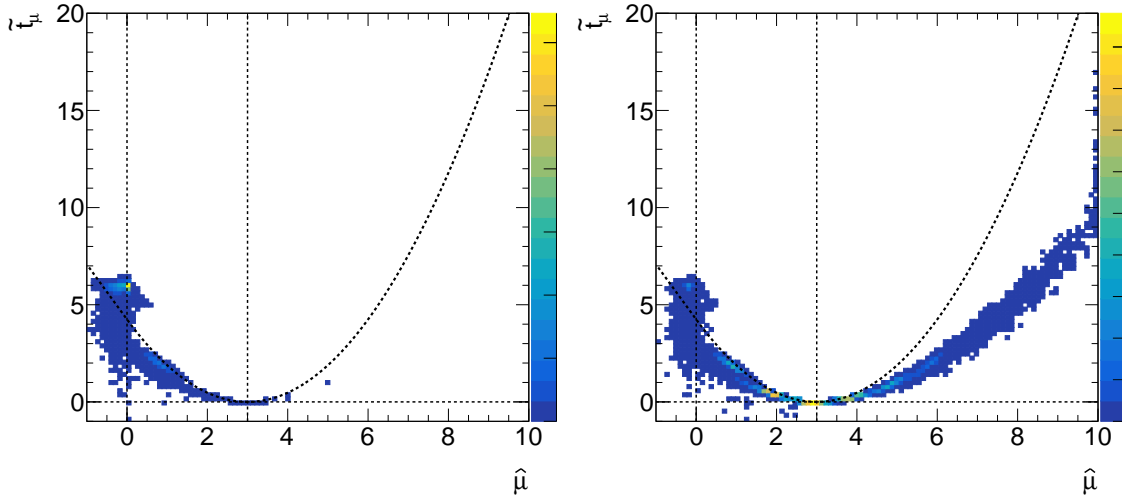


FIG. 4. The distribution of $\tilde{t}_{\hat{\mu}} : \hat{\mu}$ in Ex. 0 of Sec. IV for the hypothesized signal strength $\mu_H = 0$ (L) and $\mu_H = 3$ (R). The bold dashed curves represent the asymptotic relation from Wald's theorem.

is q_0 .

$$q_0 = \begin{cases} -2 \ln \frac{\mathcal{L}(0, \hat{\theta}(0))}{\mathcal{L}(\hat{\mu}, \hat{\theta})} & \hat{\mu} \geq 0, \\ 0 & \hat{\mu} < 0. \end{cases} \quad (4)$$

The asymptotic formulae in Ref. [3] to describe the probability distribution of these test

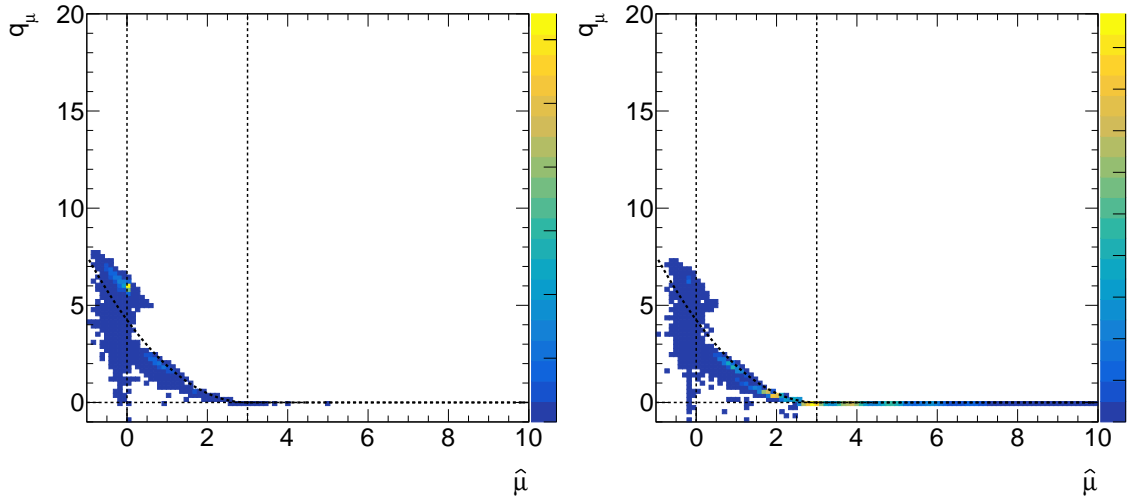


FIG. 5. The distribution of $q_\mu : \hat{\mu}$ in Ex. 0 of Sec. IV for the hypothesized signal strength $\mu_H = 0$ (L) and $\mu_H = 3$ (R). The bold dashed curves represent the asymptotic relation from Wald's theorem.

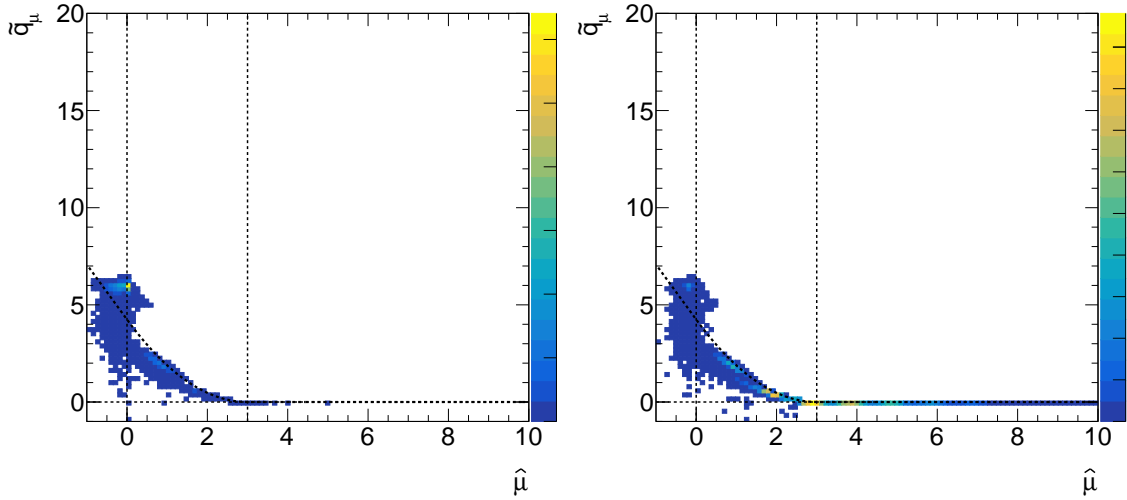


FIG. 6. The distribution of $\tilde{q}_\mu : \hat{\mu}$ in Ex. 0 of Sec. IV for the hypothesized signal strength $\mu_H = 0$ (L) and $\mu_H = 3$ (R). The bold dashed curves represent the asymptotic relation from Wald's theorem.

statistics are based on Wald's theorem [4]. It says that the logarithmic likelihood ratio, seen as a random variable, satisfies the following relation

$$t_\mu \equiv -2 \ln \lambda(\mu) = \frac{(\hat{\mu} - \mu)^2}{\sigma^2} + \mathcal{O}\left(\frac{1}{\sqrt{N}}\right), \quad (5)$$

where $\hat{\mu}$ abides by a Gaussian distribution with a mean μ_H and standard deviation σ ; and N represents the data sample size. The standard deviation σ can be obtained from either the Fisher information matrix (second-order derivatives of the logarithmic likelihood function) [6, 7] or from Wald’s theorem (Eq. 5) based on an Asimov dataset (denoted by $\sigma(\text{Wald})$). In the large sample limit, we can ignore the term $\mathcal{O}(\frac{1}{\sqrt{N}})$ in Eq. 5 (we call it “Wald’s approximation” throughout this paper). Hence we have the following asymptotic relation between the test statistics and $\hat{\mu}$.

$$q_\mu = \begin{cases} 0 & \hat{\mu} > \mu \\ \frac{(\hat{\mu}-\mu)^2}{\sigma^2} & \hat{\mu} \leq \mu \end{cases}, \quad (6)$$

$$\tilde{q}_\mu = \begin{cases} 0 & \hat{\mu} > \mu \\ \frac{(\hat{\mu}-\mu)^2}{\sigma^2} & \mu \geq \hat{\mu} \geq 0 \\ \frac{\mu^2-2\mu\hat{\mu}}{\sigma^2} & \hat{\mu} < 0 \end{cases}, \quad (7)$$

and

$$q_0 = \begin{cases} \frac{\hat{\mu}^2}{\sigma^2} & \hat{\mu} \geq 0 \\ 0 & \hat{\mu} < 0 \end{cases}. \quad (8)$$

Eventually, the probability distribution function (PDF) of these test statistics is obtained assuming that $\hat{\mu}$ abides by a Gaussian distribution.

III. NEW ASYMPTOTIC FORMULAE

The classic asymptotic formulae work very well if the sample size is not too small. To extend their usage in cases of small sample size, we have to include the contribution $\mathcal{O}(\frac{1}{\sqrt{N}})$. This is case-dependent, and we have to analyze the signal and background in each measurement. A natural idea would be to split the PDF of a test into two parts. One is described by the asymptotic formulae (with proper corrections), the other part must be case-dependent and has to be estimated in a reasonable way. This idea is inspired by the process of toy MC simulation. Imagining we are doing pseudo experiments, the “observed” number of events could be small (even 0) or large, and follows a Poisson distribution with a mean $b + \mu_H s$ where μ_H is the signal strength under the hypothesis H . Let T_μ denote a test statistic like q_μ or \tilde{q}_μ . If the “observed” number of events is larger than a threshold, its contribution to the PDF of T_μ must be well described by the classic asymptotic formula. Otherwise, we try our

best to describe its contribution in an explicit way. Fortunately, because of small statistics, the computation cost in the latter part is not big. We will see that the distribution of T_μ in the latter part is discrete and their possible values can be well predicted. Therefore, letting $f(T_\mu|\mu_H)$ be the PDF of T_μ with a hypothesized signal strength μ_H , we have

$$\begin{aligned}
f(T_\mu|\mu_H) &= \sum_{n=0}^{+\infty} f(T_\mu|n, \mu_H)P(n|b + \mu_H s) \\
&= \sum_{n=0}^{n_{\text{small}}} f(T_\mu|n, \mu_H)P(n|b + \mu_H s) + \sum_{n>n_{\text{small}}} f(T_\mu|n, \mu_H)P(n|b + \mu_H s) \\
&\approx \sum_{n=0}^{n_{\text{small}}} f_{\text{SS}}(T_\mu|n, \mu_H)P(n|b + \mu_H s) + (1 - \sum_{n=0}^{n_{\text{small}}} P(n|b + \mu_H s))f_{\text{LS}}(T_\mu|n_{\text{small}}, \mu_H(\vartheta))
\end{aligned}$$

Here $P(n|\nu)$ is Poisson distribution function; n_{small} is the boarder between large statistics (LS) and small statistics (SS), and has to be chosen appropriately. If the number of events is greater than n_{small} , the probability distribution of T_μ is described by a single function f_{LS} . f_{LS} is just the classic asymptotic formulae with a correction as explained in Sec. III C. For each possible number of events not greater than n_{small} , we obtain the probability distribution, f_{SS} , based on a simplified 6-bin distribution of the observables.

$$\begin{aligned}
f_{\text{SS}}(T_\mu|n, \mu_H) &= \sum_{k_0+k_1+k_2+k_3+k_4+k_5=n} \frac{n!}{k_0!k_1!\cdots k_5!} \prod_{i=0}^5 \left(\frac{b_i + \mu_H s_i}{b + \mu_H s}\right)^{k_i} \\
&\times f_{\text{binned}}(T_\mu|n_i = k_i, i = 0, 1, 2, 3, 4, 5; \mu_H). \quad (10)
\end{aligned}$$

Before presenting more details, here is another way to understand the new idea. Taking q_μ as example, its cumulative distribution function (CDF) is calculated below using an integral according to Wald's approximation.

$$F_{\text{Wald}}(q_\mu|\mu', \sigma) = \frac{1}{\sqrt{2\pi}\sigma} \int_{\mu - \frac{\sqrt{q_\mu}}{\sigma}}^{+\infty} e^{-\frac{1}{2}\frac{(x-\mu')^2}{\sigma^2}} dx \quad (11)$$

$$= \Phi\left(\sqrt{q_\mu} - \frac{\mu - \mu'}{\sigma}\right) \quad (12)$$

Here $\Phi(x) \equiv \frac{1}{\sqrt{2\pi}} \int_{-\infty}^x e^{-x'^2/2} dx'$. We can also calculate it in two steps (using double integrals) below

$$F_{2\text{-step}}(q_\mu|\mu', \sigma) = \frac{1}{\sqrt{2\pi}\sigma_0} \int_{-\infty}^{+\infty} e^{-\frac{1}{2}\frac{(y-\mu')^2}{\sigma_0^2}} \left[\frac{1}{\sqrt{2\pi}\sigma_1} \int_{\mu - \frac{\sqrt{q_\mu R}}{\sigma_0}}^{+\infty} e^{-\frac{1}{2}\frac{(x-y)^2}{\sigma_1^2}} dx \right] dy \quad (13)$$

$$= \Phi\left(\sqrt{q_\mu} \sqrt{\frac{\sigma_0^2 + \sigma_1^2}{\sigma_0^2}} R - \frac{\mu - \mu'}{\sqrt{\sigma_0^2 + \sigma_1^2}}\right) \quad (14)$$

We get the same result if $\sigma = \sqrt{\sigma_0^2 + \sigma_1^2}$ and $R = \frac{\sigma_0^2}{\sigma^2}$. Here σ_0 can be seen as the statistical uncertainty and y is the signal strength with considering statistical uncertainty only. σ_1 can be seen as the systematic uncertainty and x is the final signal strength with the systematic effects included. The new idea works similarly. The first step is to randomize the number of events based on a binned model without any nuisance parameter, and obtain the information on signal strength and the test statistics. The second step is to consider the systematic effects by assuming the signal strength is Gaussian-distributed with a proper spread, which is propagated to the probability distribution of the test statistics.

It is worth mentioning that there is a convolution in the calculation above. If looking at the convolution using the characteristic function method, the smearing effect from the systematic uncertainties would suppress the high-order variations in the original distribution of signal strength and test statistics, like the features due to limited sample size. Thus it explains the observation that the asymptotic formulae work better with the presence of systematic effects in Ref. [8].

To get another insight of the new idea, we introduce the following integral.

$$F_{\text{classic}}(T_\mu|\mu', \sigma_0, \sigma_1) = \frac{1}{\sqrt{2\pi}\sigma_1} \int_{\mu - \frac{\sqrt{T_\mu}}{\sigma_0}}^{+\infty} e^{-\frac{1}{2} \frac{(x-\mu')^2}{\sigma_1^2}} dx \quad (15)$$

Then we have

$$F_{\text{Wald}}(q_\mu|\mu, \sigma) = F_{\text{classic}}(q_\mu|\mu', \sigma, \sigma) \quad (16)$$

$$F_{2\text{-step}}(q_\mu|\mu, \sigma_0, \sigma_1) = \frac{1}{\sqrt{2\pi}\sigma_0} \int_{-\infty}^{+\infty} e^{-\frac{1}{2} \frac{(y-\mu')^2}{\sigma_0^2}} F_{\text{classic}}(q_\mu R|\mu', \sigma_0, \sigma_1) dy \quad (17)$$

The new idea comes in by replacing the Gaussian distribution in Eq. 17, which works well in the large sample limit, by a more precise description from a 6-bin model. Apart from this, the new idea assumes that the impact of the systematic effects is Gaussian-like and hence we can see the similarity between the two approaches (F_{classic} in the equations above).

A. A 2-bin model

In this section, we use a 2-bin model to illustrate how we obtain f_{binned} and f_{SS} because we are able to get analytic expression of the parameter of interest, namely signal strength in most measurements. Suppose the observable distribution is re-binned into only 2 bins. Let b_i , s_i and n_i denote the number of background, signal and observed events in the i -th

bin ($i = 0, 1$). They are ordered with decreasing expected significances, namely, $Z_0 > Z_1$, where Z_i is defined as

$$Z_i = 2[(b_i + \mu_H s_i) \ln(1 + \frac{\mu_H s_i}{b_i}) - \mu_H s_i]. \quad (18)$$

We further suppose the binning is made to maximize the total expected significance, $Z_{\text{tot.}} \equiv \sum_i Z_i$. So generally we have the purity in 0-th bin is greater (or even much greater) than that in the 1-th bin, $s_0/b_0 > s_1/b_1$. Given the observed number of events, n_i , and ignoring other nuisance parameters and freely-floating parameters, the optimal estimation of the signal strength is obtained by maximizing the following binned likelihood function,

$$\mathcal{L}(\mu) = \prod_{i=0}^{N_{\text{bins}}} P(n_i | b_i + \mu s_i), \quad (19)$$

or equivalently the logarithmic likelihood function,

$$\ln \mathcal{L}(\mu) = \sum_{i=0}^{N_{\text{bins}}} n_i \ln(b_i + \mu s_i) - (b_i + \mu s_i). \quad (20)$$

Where N_{bins} is the number of bins. In most of the cases, the best estimation, $\hat{\mu}$, is found such that $\partial \ln \mathcal{L} / \partial \mu = 0$, namely,

$$\sum_{i=0}^N \frac{n_i s_i}{b_i + \mu s_i} - s_i = 0. \quad (21)$$

For $N = 2$, the equation can be solved easily,

$$A = 2s_0 s_1 \quad (22)$$

$$B = s_0 b_1 + s_1 b_0 - \frac{n_0 + n_1}{s_0 + s_1} s_0 s_1 \quad (23)$$

$$C = b_0 b_1 - \frac{n_0 s_0 b_1 + n_1 s_1 b_0}{s_0 + s_1} \quad (24)$$

$$\hat{\mu}(n_0, n_1) = \frac{-B + \sqrt{B^2 - 4AC}}{2A}. \quad (25)$$

$\hat{\mu}$ as a function of n_0 and n_1 has the following feature,

$$-\frac{b_0}{s_0} = \hat{\mu}(0, n) < \hat{\mu}(1, n-1) < \hat{\mu}(2, n-2) < \dots < \hat{\mu}(n, 0) = -\frac{b_0}{s_0} + \frac{n}{s_0 + s_1}. \quad (26)$$

Especially, if $s_0/b_0 \gg s_1/b_1$, we have

$$\hat{\mu}(k, n-k) \approx -\frac{b_0}{s_0} + \frac{k}{s_0 + s_1}. \quad (27)$$

Based on the solutions above, we have three observations.

- For n number of events, there will be $n + 1$ possible values of $\hat{\mu}$.
- The possible $\hat{\mu}$ values are approximately equal-distance distributed.
- For the value $\hat{\mu}(k, n - k)$, its probability is proportional to $\frac{n!}{k!(n-k)!}$.

The observations will be confirmed in the toy MC results in Sec. IV.

Without any nuisance parameter, the distribution of $\hat{\mu}$ is discrete and the distribution of T_μ is also discrete. Taking \tilde{q}_μ as example, we have

$$\tilde{q}_\mu^{\text{binned}}(\hat{\mu}) = \begin{cases} -2[\sum_{i=0}^N n_i \ln \frac{b_i + \mu s_i}{b_i + \hat{\mu} s_i} - (\mu - \hat{\mu}) s_i], & 0 \leq \hat{\mu} < \mu \\ -2[\sum_{i=0}^N n_i \ln \frac{b_i + \mu s_i}{b_i} - \mu s_i], & \hat{\mu} < 0 \end{cases}. \quad (28)$$

However, with the presence of other nuisance parameters, we assume the distribution of $\hat{\mu}$ is Gaussian. Its mean is determined above and its standard deviation, denoted by $\sigma(\hat{\mu})$, is estimated as

$$\sigma(\hat{\mu}) = \sqrt{\sigma_0^2 + (\kappa \hat{\mu})^2}. \quad (29)$$

The motivation for this form is explained in Appendix A. Here σ_0 and κ are estimated using Asimov datasets, namely,

$$\sigma_0 = \sqrt{\sigma_A^2(\mu = 0) - \sigma_A^2(\mu = 0, \text{stat. only})} \quad (30)$$

$$\kappa = \sqrt{\sigma_A^2(\mu = \mu_H) - \sigma_A^2(\mu = \mu_H, \text{stat. only}) - \sigma_0^2 / \mu_H}, \quad (31)$$

where $\sigma_A(\mu)$ is the uncertainty of $\hat{\mu}$ from fitting to an Asimov dataset with signal strength μ ; $\sigma_A(\mu, \text{stat. only})$ is the uncertainty with fixing all other nuisance parameters. Basically, $\sigma(\hat{\mu})$ has two contributions. One does not depend upon $\hat{\mu}$ and the other does.

For simplicity, we introduce the following PDF.

$$f_{\text{classic}}(T_\mu | \mu', \sigma', \sigma) = \Phi\left(\frac{\mu' - \mu}{\sigma'}\right) \delta(T_\mu) + \begin{cases} \frac{\sigma}{2\sqrt{T_\mu}} \frac{1}{\sqrt{2\pi}\sigma'} e^{-\frac{(\mu - \sigma\sqrt{T_\mu} - \mu')^2}{2\sigma'^2}}, & T_\mu \leq \frac{\mu^2}{\sigma^2} \\ \frac{\sigma^2}{2\mu} \frac{1}{\sqrt{2\pi}\sigma'} e^{-\frac{(\frac{\mu^2 - \sigma^2 T_\mu}{2\mu} - \mu')^2}{2\sigma'^2}}, & T_\mu > \frac{\mu^2}{\sigma^2}. \end{cases} \quad (32)$$

Still taking $T_\mu = \tilde{q}_\mu$ as example, the SS part of the PDF of T_μ is

$$f_{\text{SS}}(T_\mu | n, \mu_H) = \sum_{k_0 + k_1 = n} \frac{n!}{k_0! k_1!} \left(\frac{b_0 + \mu_H s_0}{b + \mu_H s}\right)^{k_0} \left(\frac{b_1 + \mu_H s_1}{b + \mu_H s}\right)^{k_1} f_{\text{binned}}(T_\mu | n_0 = k_0, n_1 = k_1) \quad (33)$$

with

$$f_{\text{binned}}(T_\mu | n_0 = k_0, n_1 = k_1) = f_{\text{classic}}(T_\mu | \hat{\mu}(k_0, k_1), \sigma(\hat{\mu}), \sigma_{\text{Wald}}^{\text{binned}}), \quad (34)$$

$$\sigma_{\text{Wald}}^{\text{binned}} = \begin{cases} \frac{|\hat{\mu} - \mu|}{\hat{q}_\mu^{\text{binned}}(\hat{\mu})}, & \hat{\mu} > 0 \\ \sqrt{\frac{-2\mu\hat{\mu} + \mu^2}{\hat{q}_\mu^{\text{binned}}(\hat{\mu})}}, & \hat{\mu} \leq 0 \end{cases}. \quad (35)$$

It should be noted that the case of observing 0 events and the optimal $\hat{\mu}$ attained at its lowest bound will be discussed in Appendix B, respectively. Necessary corrections to $\sigma(\hat{\mu})$ will be introduced because the first-order derivation of the logarithmic likelihood does not vanish at $\hat{\mu}$.

B. A 6-bin model

In last section, we have explained the key ideas to extend the classic formulae using an observable distribution of only 2 bins. But we believe the more bins, the better performance. Considering that 5 may be arguable a safe threshold between small statistics and large statistics and also taking into account the computation time due to too many bins, it seems appropriate to use 5 bins. However, there are cases where we expect to see a large number of events but very few events in the signal-sensitive region and thus we still suffer from the effect of limited sample size. Therefore, it is necessary to deal with the large-statics part whose contribution to the signal detection is negligible. We put this part in the 6-th bin and hence propose a 6-bin model.

In practice, here is the workflow to obtain the 6-bin model.

- Merge the observable distributions in all signal regions into a fine-binning histogram for the signal and background component;
- Re-order the bins with the decreasing significance as defined in Eq. 18;
- Find the bin (denoted by i_5), the contribution of all the bins after which to the total significance is less than 0.1%. Define the signal and background yield summed over those bins as s_5 and b_5 (we use the index starting from 0).
- For the bins before i_5 , we categorize them into 5 bins and the binning is determined by maximizing the significance.

We should then update the summation in f_{SS} from the 2-bin model to the 6-bin model.

$$f_{\text{SS}}(T_\mu|n, \mu_H) = \sum_{k_0+k_1+\dots+k_5=n} \frac{n!}{k_0!k_1!\dots k_5!} \prod_{i=0}^5 \left(\frac{b_i + \mu_H s_i}{b + \mu_H s}\right)^{k_i} \times f_{\text{binned}}(T_\mu|n_0 = k_0, n_1 = k_1, \dots, n_5 = k_5). \quad (36)$$

In the end of the section, we recommend the following choice of n_{small}

$$n_{\text{small}} = \min\{b + \mu s - 1, 10\}, \quad (37)$$

with the modification of fixing b_5 at 10 and scaling s_5 to $s_5 \times 10/b_5$ if $b_5 > 10$ (b_5 is the number of background events in the region whose contribution to the signal detection is negligible). We choose n_{small} to be around $b + \mu s - 1$ because we want a conservative improvement and do not expect the updated part to be more than 50 %. However, the computation consumption is significant if $b + \mu s - 1$ is too big and hence n_{small} is capped at 10. Although the definition of n_{small} is unserious, the performance of the new formulae is robust against varying n_{small} as we will see in Sec. IV A.

It should be noted that we propose to choose 6 bins and cap b_5 and n_{small} at 10 because of the computation cost. This can be loosened and better performance is expected.

C. Three corrections and the final formulae

In this section, we apply three corrections and present the final formulae.

1. A correction to T_μ in the SS part: The simple model above is to simulate a binned measurement without any systematic uncertainty or any free parameters other than the signal strength (for example, we may have freely floating parameters to model the background in reality). This is overcome by applying a scale factor R_μ to the test value like $\tilde{q}_\mu^{\text{binned}}$ in Eq. 28. R_μ is actually the ratio of T_μ obtained from a background-only Asimov dataset to that calculated from the 6-bin model above. Taking q_μ as example, it is

$$R_\mu \equiv \frac{q_\mu^A(\mu_H = 0)}{q_\mu^{\text{binned}}(\mu_H = 0)}, \quad (38)$$

$$q_\mu^{\text{binned}}(\mu_H = 0) = -2 \sum_{i=0}^5 b_i \ln \frac{b_i + \mu s_i}{b_i} - \mu s_i, \quad (39)$$

where $q_\mu^A(\mu_H = 0)$ is the expected value of q_μ in the background-only hypothesis. In view of the Wald approximation in Eq. 5. R_μ can be seen as the ratio, $\sigma_{\text{stat.}}^2/\sigma_{\text{full}}^2$, where $\sigma_{\text{stat.}}$ is the signal strength uncertainty from the simple binned model without any systematic uncertainty while σ_{full} is that from the full measurement. This correction is already seen below Eq. 13.

2. A correction to $\sigma(\hat{\mu})$ for 0 observed events or $\hat{\mu}$ at its lowest bound: It is found that the probability of observing 0 events is significant in searching for new physics with very low background. In such cases, we cannot find $\hat{\mu}$ to make $\frac{\partial \ln \mathcal{L}}{\partial \mu}$ vanish and the optimal value is the smallest number to make the yield non-negative in all bins. The 6-bin model is able to predict the center value of T_μ well, but fail to describe its width due to systematic uncertainties. We study this case in the Appendix B and propose to use $\sigma(\hat{\mu})$ in Eq. B16 if $k_0 = k_1 = k_2 = k_3 = k_4 = 0$ in Eq. 36 and that in Eq. B17 if the optimal value $\hat{\mu}$ is at the lowest bound $-b_0/s_0$.
3. A correction to μ_H in the LS part: The SS part with the number of events not greater than n_{small} is considered in the 6-bin model. Generally, the expectation value of $\hat{\mu}$ will not be μ_H any more. To recover the right expectation value, μ_H in LS part has to be modified to be

$$\mu_H^{\text{LS}}(n_{\text{small}}, \mu_H) = \frac{\mu_H - \sum_{n \leq n_{\text{small}}} P(n|b + \mu_H s) \sum_{k_0 + \dots + k_5 = n} \frac{n!}{k_0! \dots k_5!} \prod_{i=0}^5 \left(\frac{b_i + \mu_H s_i}{b + \mu_H s} \right)^{k_i} \hat{\mu}(k_0, \dots, k_5)}{1 - \sum_{n \leq n_{\text{small}}} P(n|b + \mu_H s)} \quad (40)$$

With the three corrections, we summarize the full new formulae below for convenience.

$$f(T_\mu | \mu_H) = \sum_{n=0}^{n_{\text{small}}} f_{\text{SS}}(T_\mu | n, \mu_H) P(n|b + \mu_H s) + (1 - \sum_{n=0}^{n_{\text{small}}} P(n|b + \mu_H s)) f_{\text{LS}}(T_\mu | n_{\text{small}}, \mu_H) \quad (41)$$

$$f_{\text{SS}}(T_\mu | n, \mu_H) = \sum_{k_0 + \dots + k_5 = n} \frac{n!}{k_0! k_1! \dots k_5!} \prod_{i=0}^5 \left(\frac{b_i + \mu_H s_i}{b + \mu_H s} \right)^{k_i} f_{\text{binned}}(T_\mu | k_0, \dots, k_5; \mu_H) \quad (42)$$

$$f_{\text{LS}}(T_\mu | n_{\text{small}}, \mu_H) = f_{\text{classic}}(T_\mu | \mu_H^{\text{LS}}(n_{\text{small}}, \mu_H), \sigma_{\text{Wald}}, \sigma_{\text{Wald}}) \quad (43)$$

$$f_{\text{binned}}(T_\mu | k_0, \dots, k_5) = f_{\text{classic}}(T_\mu | \hat{\mu}(k_0, \dots, k_5), \sigma(\hat{\mu}), \sigma_{\text{Wald}}^{\text{binned}}). \quad (44)$$

Here (taking q_μ and \tilde{q}_μ as example)

$$\sigma_{\text{Wald}} = \frac{\mu}{\sqrt{q_\mu^A(\mu_H = 0)}} \quad (45)$$

$$\sigma(\hat{\mu}) = \begin{cases} \kappa \frac{\mu - c\hat{\mu}}{2}, & \text{if } k_0 = \dots = k_4 = 0 \\ \sqrt{\sigma_0^2 + (\kappa\hat{\mu})^2 + (\kappa \frac{\mu - c\hat{\mu}}{2})^2}, & \text{if } \hat{\mu} = -b_0/s_0 \\ \sqrt{\sigma_0^2 + (\kappa\hat{\mu})^2}, & \text{otherwise} \end{cases} \quad (46)$$

$$\sigma_{\text{Wald}}^{\text{binned}} = \begin{cases} \frac{|\hat{\mu} - \mu|}{\sqrt{R_\mu \tilde{q}_\mu^{\text{binned}}(\hat{\mu})}}, & \hat{\mu} > 0 \\ \frac{-2\mu\hat{\mu} + \mu^2}{\sqrt{R_\mu \tilde{q}_\mu^{\text{binned}}(\hat{\mu})}}, & \hat{\mu} \leq 0 \end{cases} \quad (47)$$

$$\tilde{q}_\mu^{\text{binned}}(\hat{\mu}) = \begin{cases} -2[\sum_{i=0}^5 n_i \ln \frac{b_i + \mu s_i}{b_i + \hat{\mu} s_i} - (\mu - \hat{\mu})s_i], & \hat{\mu} > 0 \\ -2[\sum_{i=0}^5 n_i \ln \frac{b_i + \mu s_i}{b_i} - \mu s_i], & \hat{\mu} \leq 0 \end{cases} \quad (48)$$

$$n_{\text{small}} = \min\{b + \mu s - 1, 10\}, \quad (49)$$

where $c = 1$ for q_μ and 2 for \tilde{q}_μ ; R_μ is defined in Eq. 38; $\mu_H^{\text{LS}}(n_{\text{small}}, \mu_H)$ is defined in Eq. 40; $\hat{\mu}(k_1, \dots, k_5)$ is obtained by maximizing the binned likelihood function in Eq. 19.

IV. TWO EXAMPLES

In this section, we apply the new formulae to two examples to compare the performance of the classic and new asymptotic formulae. They are denoted by Ex. 0 and Ex. 1 with increasing sample size. The physics behind the examples is to measure Higgs production cross section using the $H \rightarrow \gamma\gamma$ mode. The signal strength is obtained by fitting to the $\gamma\gamma$ invariant mass spectrum. Table II summarizes the expected signal and background yields in the mass region $123 < m(\gamma\gamma) < 127$ GeV. The expected background and signal yields are low in both examples. The signal shape is simulated by a Gaussian distribution while the background shape is simulated by an exponential distribution. They are shown in Fig. 7. According to the strategy in Sec. IIIB, the 6-bin model is built and the expected yield in each bin in the background-only hypothesis is shown in Table III. It should be emphasized that these numbers vary under different hypotheses.

We further consider three systematic uncertainties. They are due to the luminosity measurement, our knowledge on Higgs mass and the spurious signal, the last of which directly affects the expected signal yield and is usually dominant in real analyses [9]. The uncertainty sizes are summarized in Table IV. In addition, three ‘‘observed’’ data samples

TABLE II. Summary of the yields expected in the mass region $123 < m(\gamma\gamma) < 127$ GeV in the two examples.

Yield	signal background	
Ex. 0	0.91	0.64
Ex. 1	0.91	2.79

TABLE III. The signal and background yields in the 6-bin model.

	Bin	0	1	2	3	4	5
Ex. 0	sig.	0.571	0.194	0.122	0.066	0.038	0.010
	bkg.	0.146	0.070	0.068	0.067	0.098	2.98
Ex. 1	sig.	0.571	0.194	0.122	0.066	0.038	0.010
	bkg.	0.328	0.163	0.162	0.161	0.240	7.514

with increasing injected signal strength are also prepared for each example. The injected signal strength is negative (-0.15 in Ex. 0 and -0.5 in Ex. 1), $+0.5$ and $+2$, respectively.

First of all, let us investigate asymptotic relation between \tilde{q}_μ and $\hat{\mu}$ in Eq. 7 using the toy simulations. Figure 6 and 8 are the scattering plot of $\tilde{q}_\mu : \hat{\mu}$ in Ex. 0 and Ex. 1. On the one hand, we can see that the asymptotic form still looks good even in these low-statistics cases. On the other hand, there are clear structures which reflect the discrete feature in the distribution of \tilde{q}_μ or $\hat{\mu}$.

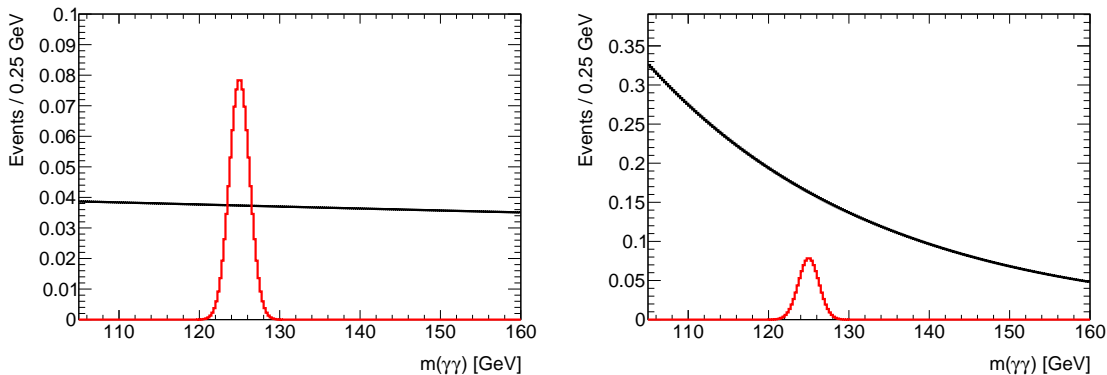


FIG. 7. The distribution of $m(\gamma\gamma)$ in Ex. 0 (L) and Ex. 1 (R). The red histograms represent the signal and the black histograms represent the background.

TABLE IV. Summary of systematic uncertainties.

	Luminosity	Higgs mass	Spurious signal
Uncertainty	$\pm 2\%$	$\pm 0.2 \text{ GeV}$	$\pm 15\%$

Secondly, let us investigate the discrete features. For the toy simulations with observing 4 events, the distribution of $\hat{\mu}$ and \tilde{q}_μ in Ex. 0 is shown in Fig. 9 and Fig. 10, respectively. We can see 5 equal-distance peaks in the $\hat{\mu}$ distribution (mostly visible in right plot of Fig. 9). They also follow the binomial distribution approximately. This confirms the three observations in Sec. III A. Furthermore, we can see the prediction from the 6-bin model agrees better with the toy results than the 2-bin model.

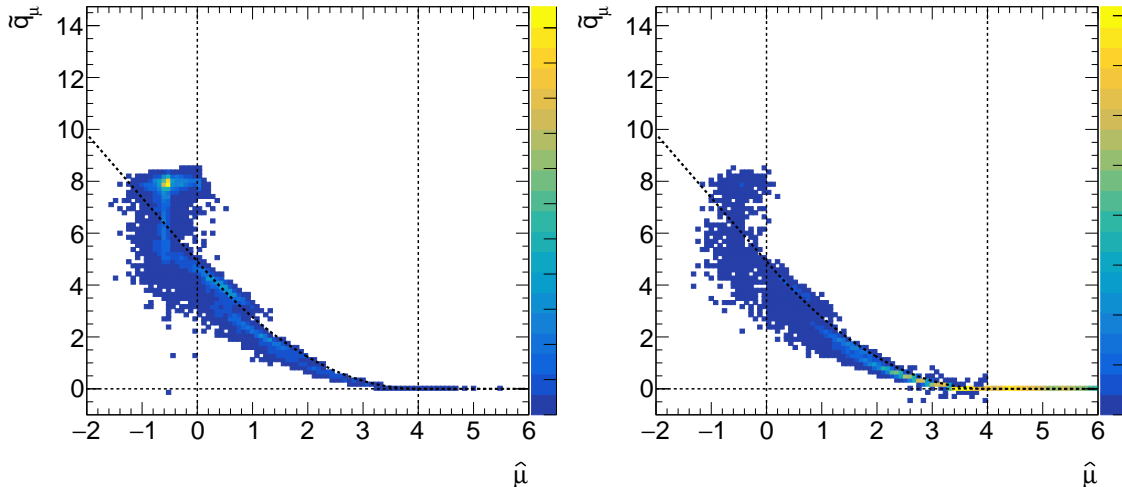


FIG. 8. The scattering plot of $\tilde{q}_\mu : \hat{\mu}$ with $mu = 4$ in Ex. 1 from the toy experiments under the hypothesis $\mu_H = 0$ (L) and $\mu_H = \mu = 4$ (R). The bold dashed curve shows the asymptotic formulae according to Wald’s theorem.

Finally, Fig. 11 12 and 13 show the distributions of \tilde{q}_μ from the toy simulations in Ex. 0 and Ex. 1 for different test signal strengths and “observed” datasets as well as the predicted distributions from the classic and new formulae. It is clear that new formulae are able to describe the discrete feature due to the low statistics. In Fig. 14, we show CLs [10, 11] as a function of μ and also upper limits at 95 % confidence level (C.L.) for different observed datasets. The limits are further compared in Fig. 17. Indeed, the new formulae outperform the classic ones.

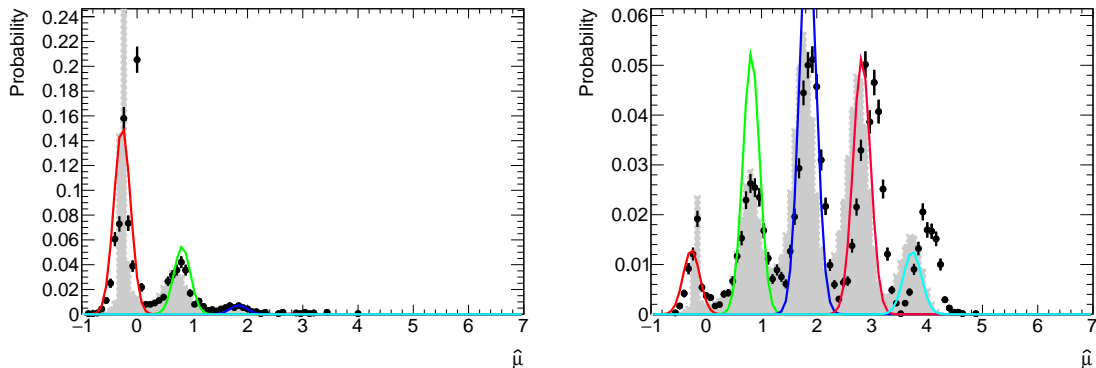


FIG. 9. The distribution of $\hat{\mu}$ in Ex. 0 under the hypothesis $\mu_H = 0$ (L) and $\mu_H = \mu = 3$ (R) for the number of total events being 4. The black dots represent the toy experiments. The curves with different colors represent the solutions predicted in the 2-bin model. The gray histograms are the prediction from the 6-bin model.

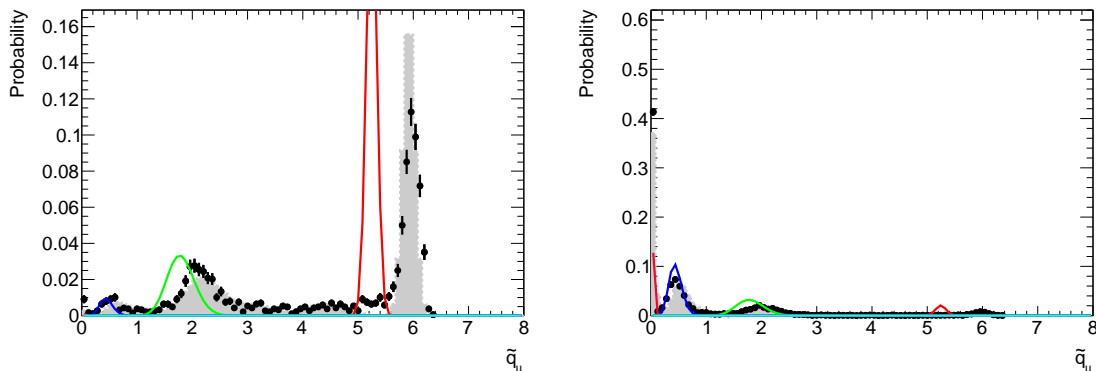


FIG. 10. The distribution of \tilde{q}_μ in Ex. 0 under the hypothesis $\mu_H = 0$ (L) and $\mu_H = \mu = 3$ (R) for the number of total events being 4. The black dots represent the toy experiments. The curves with different colors represent the solutions predicted in the 2-bin model. The gray histograms are the prediction from the 6-bin model.

A. The effect of the choice of n_{small}

In Sec. III, n_{small} for the hypothesis μ_H is proposed to be $b + \mu s - 1$. This choice is based on some plausible reasons and conservative. In this section, we try different choices and check if the upper limits are robust. Since the background yield is 0.64 (2.79) in Ex. 0 (Ex. 1) in Table II, we vary n_{small} by from -1 up to +5. Figure 15 and 16 are some examples

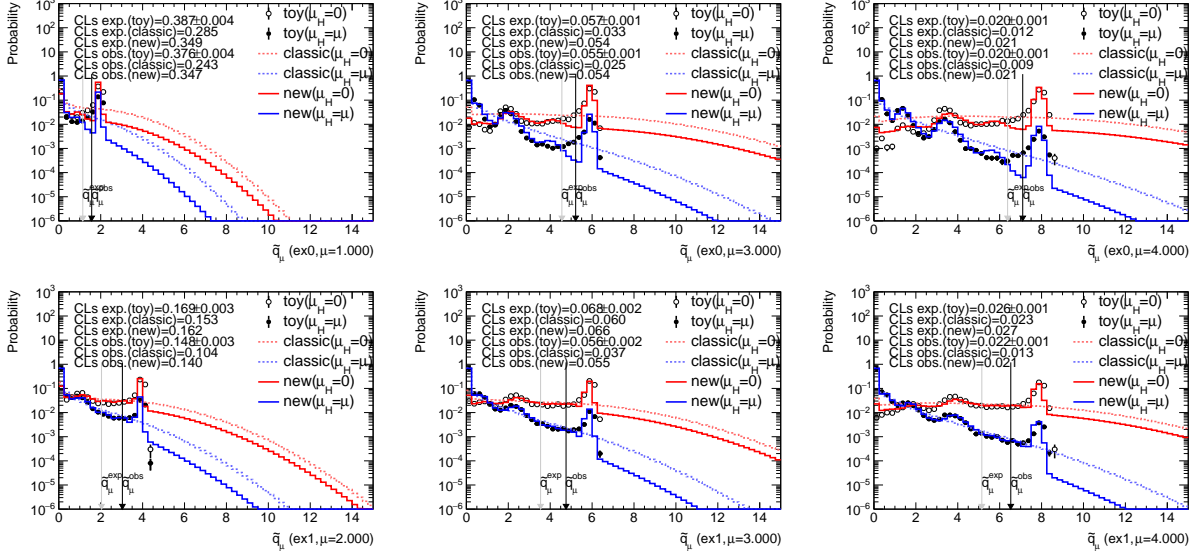


FIG. 11. The probability distributions of \tilde{q}_μ in Ex. 0 (Top row) and Ex. 1 (Bottom row) for an “observed” dataset with a negative signal strength. The black dots and open circles represent the toy MC results. The blue/red solid histograms represent the new asymptotic formulae in this work while the blue/red dashed histograms represent the classic asymptotic formulae from Wald’s approximation. The black and gray arrows represent the observed and expected \tilde{q}_μ , respectively.

of \tilde{q}_μ distribution for different n_{small} choices. The upper limit difference with respect to the toy results as a function of n_{small} is summarized in Fig. 17. We can see that upper limits predicted from the new formulae are stable.

B. The test statistic q_μ

In this section, we present the upper limits using q_μ instead. It differs from \tilde{q}_μ only when $\hat{\mu}$ is negative. Figure 18 shows some examples of q_μ distribution. Figure 19 shows the upper limits. We can see the new formulae are generally better.

C. The test statistic q_0

In this section, we consider the test statistic q_0 , which is used to establish the discovery of a signal. Figure 20 and 21 show the distribution of q_0 in Ex. 0 and Ex. 1 respectively for different observed datasets. For comparison, we also show the significance Z as a function

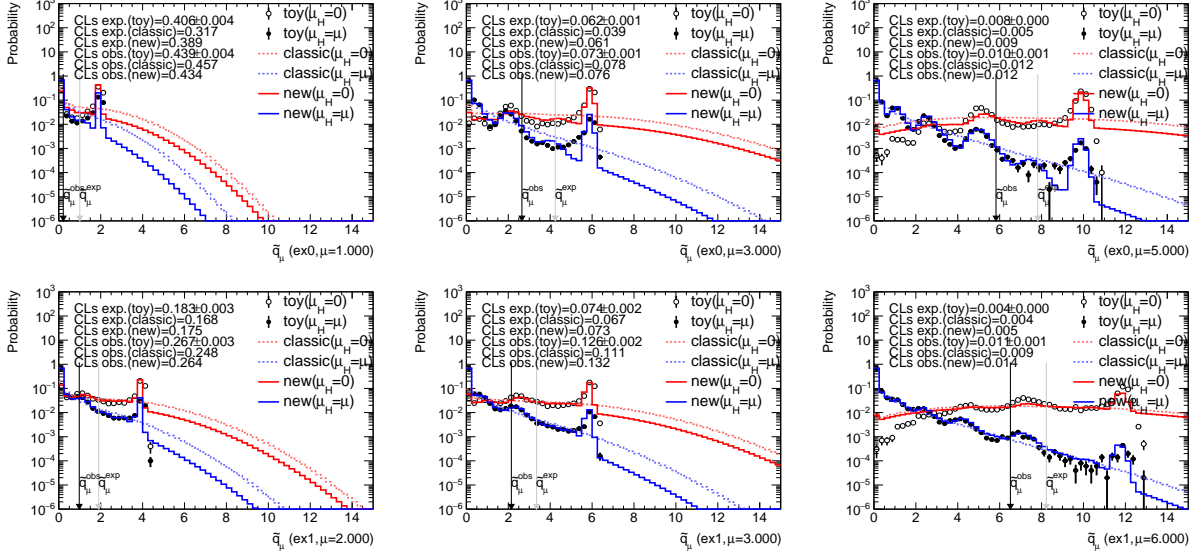


FIG. 12. The probability distributions of \tilde{q}_μ in Ex. 0 (Top row) and Ex. 1 (Bottom row) for an “observed” dataset with signal strength equal to 0.5. The black dots and open circles represent the toy MC results. The blue/red solid histograms represent the new asymptotic formulae in this work while the blue/red dashed histograms represent the classic asymptotic formulae from Wald’s approximation. The black and gray arrows represent the observed and expected \tilde{q}_μ , respectively.

of possible observed value of q_0 although there is a unique value in each case. Using the classic asymptotic formulae, we have $Z = \sqrt{q_0}$. From these plots, it is clear that the new formulae work better.

V. SUMMARY

In this work, we try to improve the classic asymptotic formulae to describe the probability distribution of the likelihood-ratio statistical tests which are commonly used in the field of high energy physics. The idea is to split the PDF into two parts. One is described by the classic formulae with proper corrections, and the other is calculated by mimicking the process of toy MC simulation. This idea successfully predicts the discrete features in the small-statistics cases. Examples with different sample sizes and different “observed” datasets are presented and show that the new formulae have stable improvements on both the differential distribution of the test statistic, the upper limit and significance calculations.

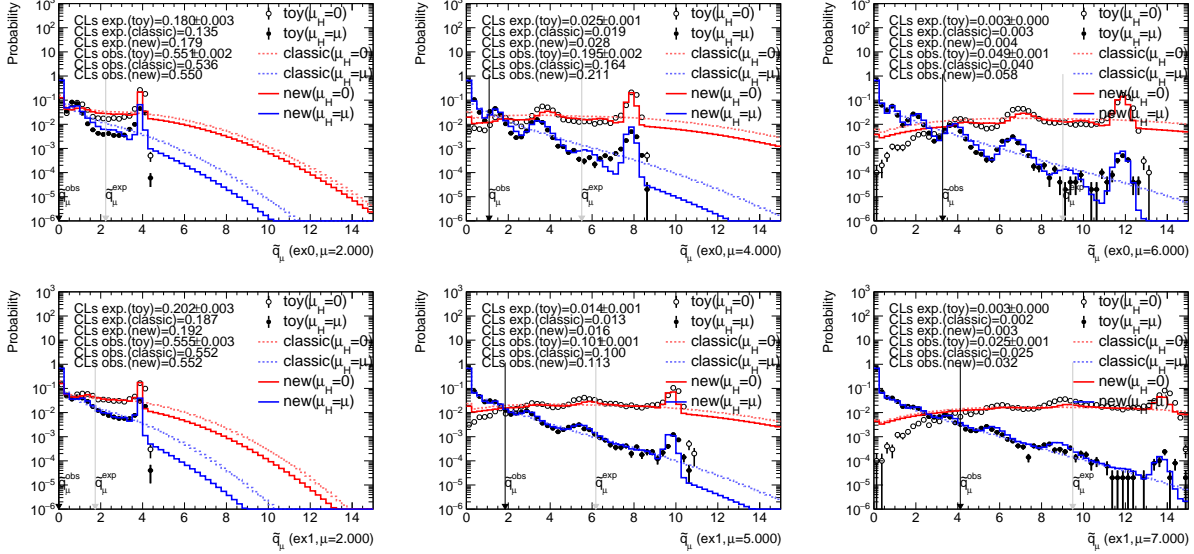


FIG. 13. The probability distributions of \tilde{q}_μ in Ex. 0 (Top row) and Ex. 1 (Bottom row) for an “observed” dataset with signal strength equal to 2. The black dots and open circles represent the toy MC results. The blue solid/dashed histograms represent the new asymptotic formulae in this work while the red solid/dashed histograms represent the classic asymptotic formulae from Wald’s approximation. The black and gray arrows represent the observed and expected \tilde{q}_μ , respectively.

ACKNOWLEDGMENTS

L.G. Xia would like to thank Fang Dai for her encouragement and partial financial support. This work is supported by the Young Scientists Fund of the National Natural Science Foundation of China (Grant No. 12105140).

Appendix A: Motivation for the uncertainty breaking

For a binned measurement with N_{bins} bins, let b_i , s_i and n_i be the number of predicted background events, signal events and observed events in the i -th bin, respectively. Introducing one signal systematic uncertainty δ_i and one background systematic uncertainty Δ_i with the corresponding nuisance parameter α and β , the logarithmic likelihood function is

$$\ln \mathcal{L}(\mu, \alpha, \beta) = \sum_{i=1}^{N_{\text{bins}}} [n_i \ln(b_i(1 + \beta\Delta_i) + \mu s_i(1 + \alpha\delta_i)) - (b_i(1 + \beta\Delta_i) + \mu s_i(1 + \alpha\delta_i))] - \frac{\alpha^2}{2} - \frac{\beta^2}{2}, \quad (\text{A1})$$

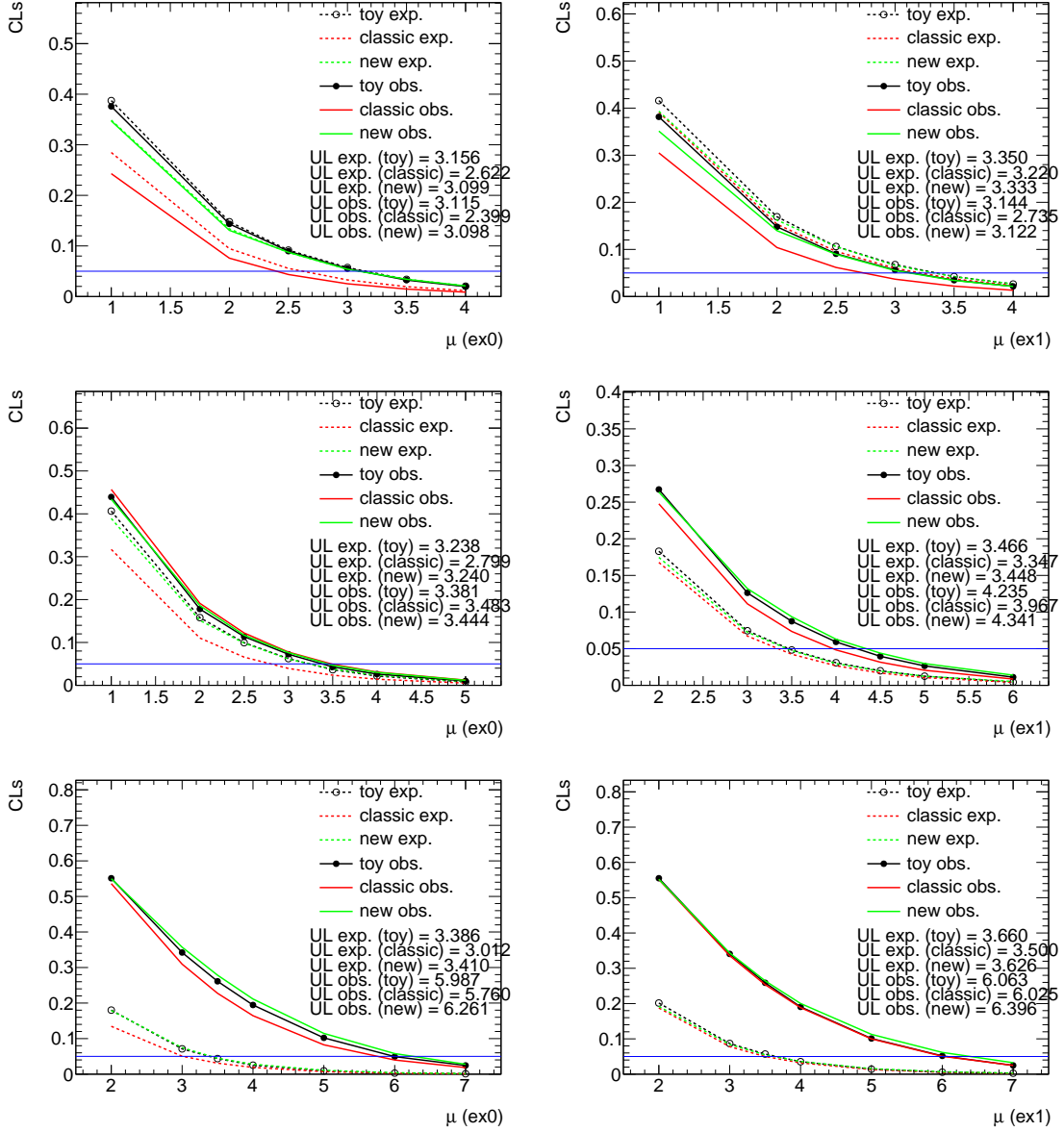


FIG. 14. CLs as a function of μ in Ex. 0 (L) and Ex. 1 (R) using the test statistic \tilde{q}_μ . From top to bottom, they represent different observed datasets. The black curves with markers show the toy MC results. The red and green curves are the predictions from the classic and new asymptotic formulae, respectively.

where the last two terms are due to the Gaussian constraints. For an Asimov dataset $n_i = b_i + \mu s_i$, let the partial derivatives $\frac{\partial \ln \mathcal{L}}{\partial \mu}$, $\frac{\partial \ln \mathcal{L}}{\partial \alpha}$ and $\frac{\partial \ln \mathcal{L}}{\partial \beta}$ vanish to reach the maximum likelihood. We obtain

$$\hat{\mu} = \mu, \quad \hat{\alpha} = 0, \quad \hat{\beta} = 0. \quad (\text{A2})$$

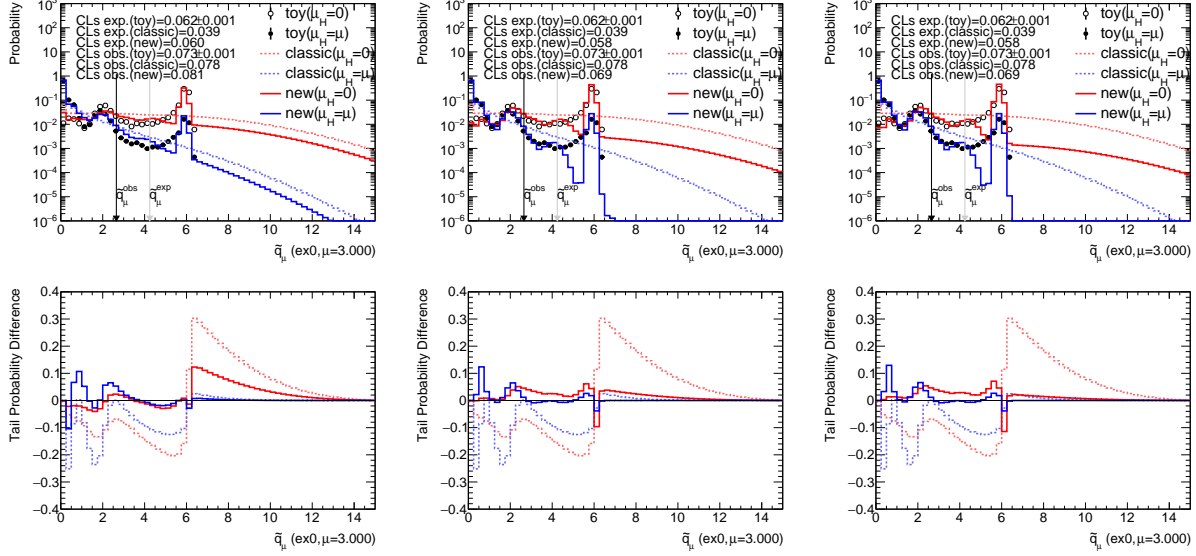


FIG. 15. Top: the probability distributions of \tilde{q}_μ in Ex. 0. From left to right, n_{small} is the nominal value -1 , $+3$ and $+5$, respectively. Bottom: the relative difference of the tail probability with respect to the toy results (for better visibility, the relative difference for the hypothesis $\mu_H = \mu$ is scaled by a factor of 5). The black dots and open circles represent the toy MC results. The blue/red solid histograms represent the new asymptotic formulae in this work while the blue/red dashed histograms represent the classic asymptotic formulae from Wald's approximation. The black and gray arrows represent the observed and expected \tilde{q}_μ , respectively.

Now we evaluate the Hessian matrix elements at these optimal values. For simplicity, we introduce $\tilde{\Delta}_i \equiv b_i \Delta_i$, $\tilde{\delta}_i \equiv s_i \delta_i$, and the symbol \otimes , which is defined as

$$A \otimes B \equiv \sum_{i=1}^{N_{\text{bins}}} \frac{A_i B_i}{n_i}. \quad (\text{A3})$$

The Hessian matrix elements are then

$$\begin{aligned} -\frac{\partial^2 \ln \mathcal{L}}{\partial \mu^2} &= s \otimes s, & -\frac{\partial^2 \ln \mathcal{L}}{\partial \mu \partial \alpha} &= (s \otimes \tilde{\delta})\mu, & -\frac{\partial^2 \ln \mathcal{L}}{\partial \mu \partial \beta} &= (s \otimes \tilde{\Delta}) \\ -\frac{\partial^2 \ln \mathcal{L}}{\partial \alpha^2} &= (\tilde{\delta} \otimes \tilde{\delta})\mu^2 + 1, & -\frac{\partial^2 \ln \mathcal{L}}{\partial \alpha \partial \beta} &= (\tilde{\delta} \otimes \tilde{\Delta})\mu, & -\frac{\partial^2 \ln \mathcal{L}}{\partial \beta^2} &= \tilde{\Delta} \otimes \tilde{\Delta} + 1. \end{aligned} \quad (\text{A4})$$

Let \mathbf{H} denote the Hessian matrix. It can be written as a sum of two matrices, \mathbf{A} and \mathbf{B} .

$$\mathbf{A} = \begin{pmatrix} s \otimes s & 0 & 0 \\ 0 & 1 & 0 \\ 0 & 0 & 1 \end{pmatrix}, \quad \mathbf{B} = \begin{pmatrix} 0 & (s \otimes \tilde{\delta})\mu & s \otimes \tilde{\Delta} \\ (s \otimes \tilde{\delta})\mu & (\tilde{\delta} \otimes \tilde{\delta})\mu^2 & (\tilde{\delta} \otimes \tilde{\Delta})\mu \\ (s \otimes \tilde{\Delta}) & (\tilde{\delta} \otimes \tilde{\Delta})\mu & \tilde{\Delta} \otimes \tilde{\Delta} \end{pmatrix}. \quad (\text{A5})$$

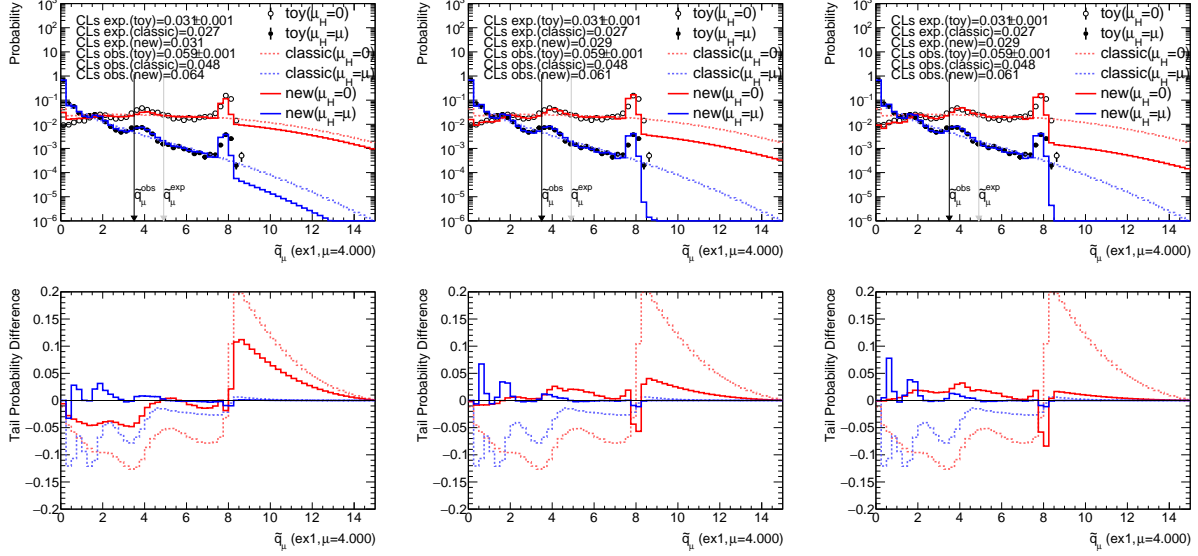


FIG. 16. Top: the probability distributions of \tilde{q}_μ in Ex. 1. From left to right, n_{small} is the nominal value -1 , $+3$ and $+5$, respectively. Bottom: the relative difference of the tail probability with respect to the toy results (for better visibility, the relative difference for the hypothesis $\mu_H = \mu$ is scaled by a factor of 5). The black dots and open circles represent the toy MC results. The blue/red solid histograms represent the new asymptotic formulae in this work while the blue/red dashed histograms represent the classic asymptotic formulae from Wald's approximation. The black and gray arrows represent the observed and expected \tilde{q}_μ , respectively.

Let \mathbf{V} denote the covariance matrix for μ , α and β . We have $\mathbf{V} = \mathbf{H}^{-1} = (\mathbf{A} + \mathbf{B})^{-1} = (\mathbf{1} + \mathbf{A}^{-1}\mathbf{B})^{-1}\mathbf{A}^{-1}$. Assuming all systematic uncertainties are small, we can approximate \mathbf{V} using the following trick [7]

$$\mathbf{1} = (\mathbf{1} + \mathbf{x})(\mathbf{1} - \mathbf{x} + \mathbf{x}^2 - \dots), \quad (\text{A6})$$

where $\mathbf{1}$ is the unit matrix. Hence we have

$$\mathbf{V} = (\mathbf{1} + \mathbf{A}^{-1}\mathbf{B})^{-1}\mathbf{A}^{-1} \approx (\mathbf{1} - \mathbf{A}^{-1}\mathbf{B} + (\mathbf{A}^{-1}\mathbf{B})^2)\mathbf{A}^{-1}, \quad (\text{A7})$$

and the uncertainty of the signal strength, σ_μ , is approximately

$$\sigma_\mu^2 = \mathbf{V}_{11} \approx \frac{1}{s \otimes s} + \left(\frac{s \otimes \tilde{\Delta}}{s \otimes s} \right)^2 + \left(\frac{s \otimes \tilde{\delta}}{s \otimes s} \right)^2 \mu^2, \quad (\text{A8})$$

where the first term is the statistical uncertainty, the second term is due to the background systematic uncertainty and the third term is due to the signal systematic uncertainty. This

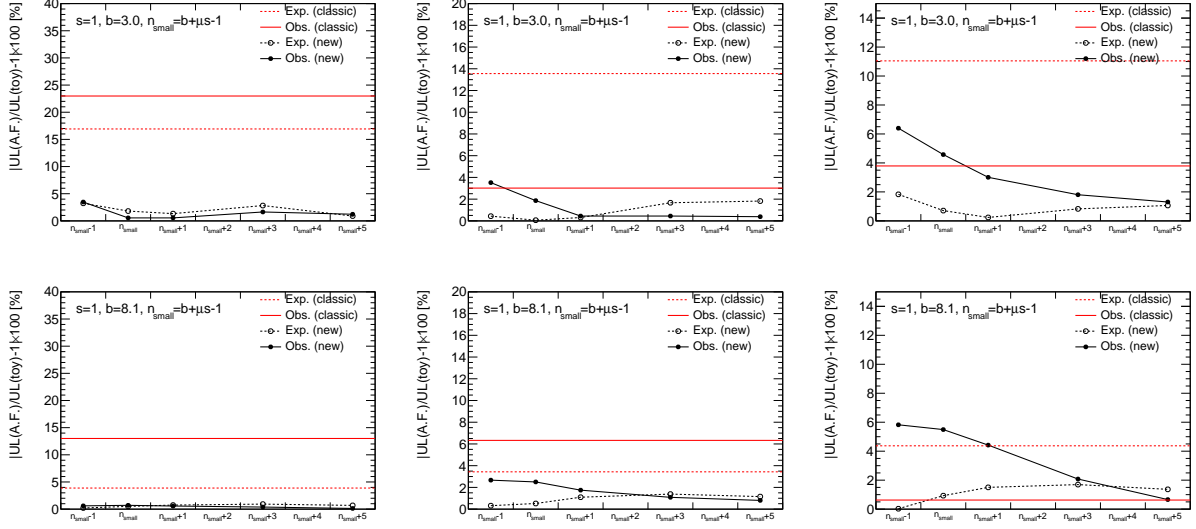


FIG. 17. The relative difference of upper limit compared to the toy results as a function of the choice of n_{small} in Ex. 0 (Top) and Ex. 1 (Bottom). From left to right, they correspond to an observed data with a negative signal strength, $\mu = 0.5$, and $\mu = 2$.

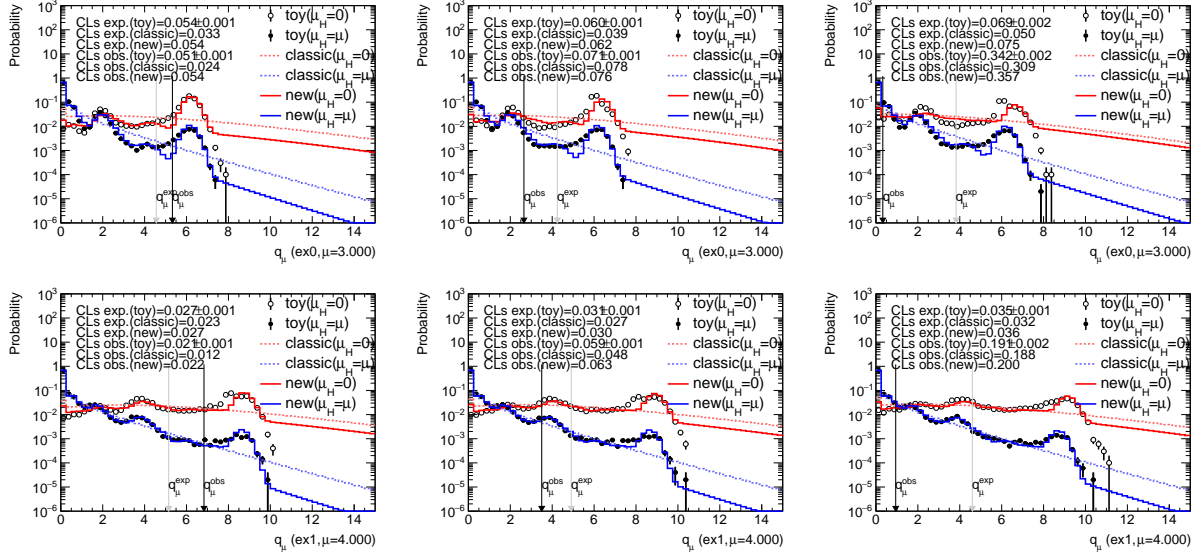


FIG. 18. The probability distributions of q_μ in Ex. 0 (Top) and Ex. 1 (Bottom). From left to right, different data sets are used. The black dots and open circles represent the toy MC results. The blue/red solid histograms represent the new asymptotic formulae in this work while the blue/red dashed histograms represent the classic asymptotic formulae from Wald's approximation. The black and gray arrows represent the observed and expected q_μ , respectively.

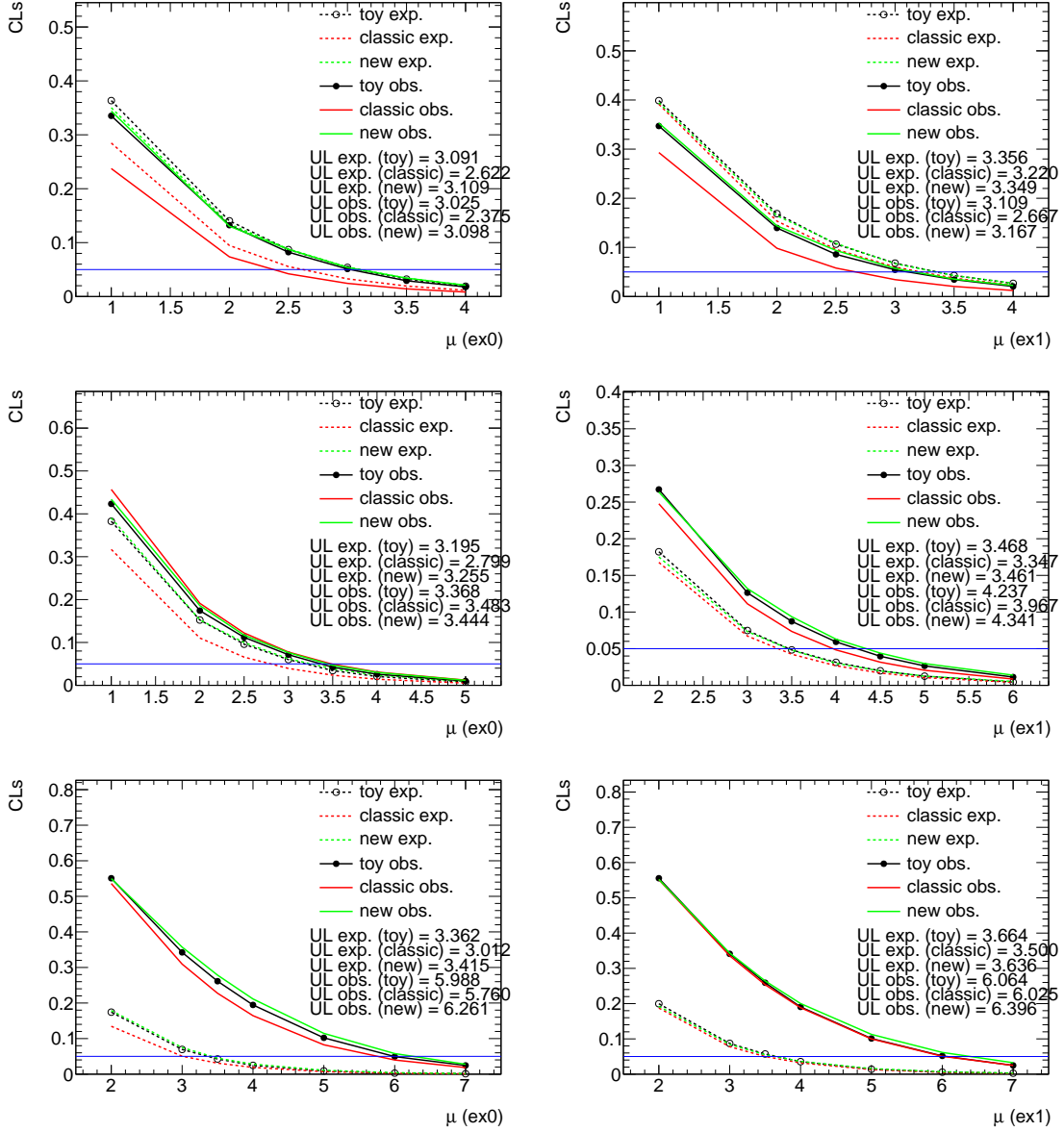


FIG. 19. CLs as a function of μ in Ex. 0 (L) and Ex. 1 (R) using the test statistic q_μ . From top to bottom, they represent different observed datasets. The black curves with markers show the toy MC results. The red and green curves are the predictions from the classic and new asymptotic formulae, respectively.

is the motivation for the form in Eq. 29 and hence the following relation.

$$\sigma_0 = \frac{s \otimes \tilde{\Delta}}{s \otimes s}, \quad \kappa = \frac{s \otimes \tilde{\delta}}{s \otimes s}. \quad (\text{A9})$$

It is of no difficulty to extend to the case of multiple signal and background systematic uncertainties, and the same conclusion holds in the sense that all systematic uncertainties

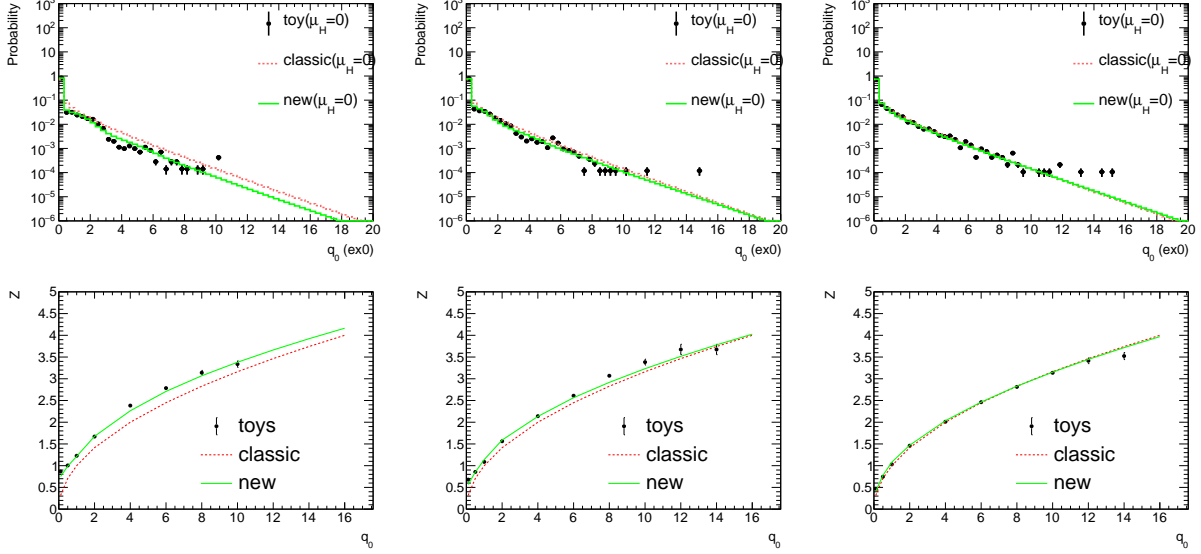


FIG. 20. Top: the probability distributions of q_0 in Ex. 0. Bottom: the significance Z as a function of a possible observed value of q_0 . From left to right, it represents different observed datasets with increasing input signal strength. The black dots represent the toy MC results. The green solid histograms represent the new asymptotic formulae in this work while the red dashed histograms represent the classic asymptotic formulae from Wald’s approximation.

are small. For better explanation in next appendix and supposing we have N_{sys}^S signal systematic uncertainties, κ becomes

$$\kappa = \sqrt{\sum_{k=1}^{N_{\text{sys}}^S} \left(\frac{s \otimes \tilde{\delta}^k}{s \otimes s} \right)^2}, \quad (\text{A10})$$

where $s \otimes \tilde{\delta}^k = \sum_{i=1}^{N_{\text{bins}}} \frac{s_i s_i \delta_i^k}{n_i}$ with δ_i^k being the effect of the k -th signal uncertainty on the i -th bin. If the uncertainties only affect the yield, we have δ_i^k is the same for i (written as δ^k) and

$$\kappa = \sqrt{\sum_{k=1}^{N_{\text{sys}}^S} (\delta^k)^2}. \quad (\text{A11})$$

Appendix B: Likelihood-ratio tests in the case of 0 events

The probability of observing 0 events is significant in searching for new physics with low background. The likelihood-ratio tests may behavior very differently in this extreme case. Therefore, we consider it dedicatedly in this appendix. For a binned measurement with

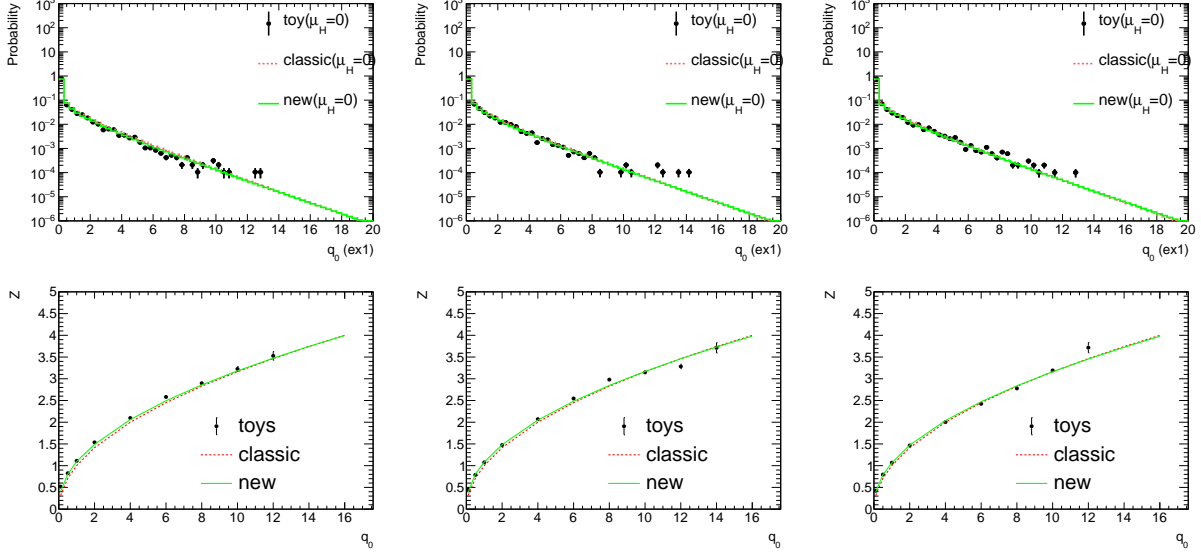


FIG. 21. Top: the probability distributions of q_0 in Ex. 1. Bottom: the significance Z as a function of a possible observed value of q_0 . From left to right, it represents different observed datasets with increasing input signal strength. The black dots represent the toy MC results. The green solid histograms represent the new asymptotic formulae in this work while the red dashed histograms represent the classic asymptotic formulae from Wald's approximation.

N_{sys}^B background systematic uncertainties and N_{sys}^S signal systematic uncertainties, the logarithmic likelihood function is

$$\ln \mathcal{L}(\mu, \theta_1, \alpha_1, \dots) = \sum_{i=1}^{N_{\text{bins}}} [n_i \ln \nu_i(\mu, \theta_1, \alpha_1, \dots) - \nu_i(\mu, \theta_1, \alpha_1, \dots)] - \sum_{j=1}^{N_{\text{sys}}^B} \frac{(\theta_j - \bar{\theta}_j)^2}{2} - \sum_{k=1}^{N_{\text{sys}}^S} \frac{(\alpha_k - \bar{\alpha}_k)^2}{2}, \quad (\text{B1})$$

with

$$\nu_i(\mu, \theta_1, \alpha_1, \dots) \equiv b_i \left(1 + \sum_{j=1}^{N_{\text{sys}}^B} \theta_j \Delta_i^j\right) + \mu s_i \left(1 + \sum_{k=1}^{N_{\text{sys}}^S} \alpha_k \delta_i^k\right). \quad (\text{B2})$$

Here N_{bins} is the number of bins; b_i and s_i are the expected number of background and signal events, respectively; n_i is the observed number of events; Δ_i^j (δ_i^k) is the effect in the i -th bin due to the j -th background (the k -th signal) systematic uncertainty; θ_j s and α_k s are the nuisance parameters while $\bar{\theta}_j$ s and $\bar{\alpha}_k$ s are auxiliary data in the toy experiment generation. The last two terms are due to Gaussian constraint.

To reach the maximum likelihood, we investigate the partial derivatives $\frac{\partial \ln \mathcal{L}}{\partial \theta_j}$, $\frac{\partial \ln \mathcal{L}}{\partial \alpha_k}$ and $\frac{\partial \ln \mathcal{L}}{\partial \mu}$. For the unconditional fit, we have

$$\frac{\partial \ln \mathcal{L}}{\partial \theta_j} = \sum_{i=1}^{N_{\text{bins}}} \frac{n_i b_i \Delta_i^j}{\nu_i(\mu, \theta_1, \alpha_1, \dots)} - b_i \Delta_i^j - (\theta_j - \bar{\theta}_j), \quad (\text{B3})$$

$$\frac{\partial \ln \mathcal{L}}{\partial \alpha_k} = \sum_{i=1}^{N_{\text{bins}}} \frac{n_i \mu s_i \delta_i^k}{\nu_i(\mu, \theta_1, \alpha_1, \dots)} - \mu s_i \delta_i^k - (\alpha_k - \bar{\alpha}_k), \quad (\text{B4})$$

$$\frac{\partial \ln \mathcal{L}}{\partial \mu} = \sum_{i=1}^{N_{\text{bins}}} \frac{n_i s_i (1 + \sum_{k=1}^{N_{\text{sys}}^S} \alpha_k \delta_i^k)}{\nu_i(\mu, \theta_1, \alpha_1, \dots)} - s_i (1 + \sum_{k=1}^{N_{\text{sys}}^S} \alpha_k \delta_i^k). \quad (\text{B5})$$

We only consider the case of 0 events in all bins, namely, $n_1 = n_2 = \dots = 0$. $\frac{\partial \ln \mathcal{L}}{\partial \mu}$ is assumed to be negative as it is true for small signal uncertainties. The optimal values satisfy

$$\hat{\theta}_j = \bar{\theta}_j - \sum_{i=1}^{N_{\text{bins}}} b_i \Delta_i^j \quad (j = 1, 2, \dots, N_{\text{sys}}^B), \quad (\text{B6})$$

$$\hat{\alpha}_j = \bar{\alpha}_k - \hat{\mu} \sum_{i=1}^{N_{\text{bins}}} s_i \delta_i^k \quad (j = 1, 2, \dots, N_{\text{sys}}^S), \quad (\text{B7})$$

$$\hat{\mu} = \max \left\{ -\frac{b_1 (1 + \sum_{j=1}^{N_{\text{sys}}^B} \hat{\theta}_j \Delta_1^j)}{s_1 (1 + \sum_{k=1}^{N_{\text{sys}}^S} \hat{\alpha}_k \delta_1^k)}, -\frac{b_2 (1 + \sum_{j=1}^{N_{\text{sys}}^B} \hat{\theta}_j \Delta_2^j)}{s_2 (1 + \sum_{k=1}^{N_{\text{sys}}^S} \hat{\alpha}_k \delta_2^k)}, \dots \right\}. \quad (\text{B8})$$

Since $\frac{\partial \ln \mathcal{L}}{\partial \mu} < 0$, we choose $\hat{\mu}$ to be smallest value to make the expected number of events non-negative in all bins. For the conditional fit with μ fixed, the optimal value are

$$\hat{\hat{\theta}}_j(\mu) = \hat{\theta}_j, \quad (\text{B9})$$

$$\hat{\hat{\alpha}}_k(\mu) = \bar{\alpha}_k + \frac{\mu}{\hat{\mu}} (\hat{\alpha}_k - \bar{\alpha}_k) \quad (j = 1, 2, \dots, N_{\text{sys}}^S). \quad (\text{B10})$$

We find that $\hat{\hat{\theta}}_j(\mu)$ is the same as $\hat{\theta}_j$ and independent on the value of μ . This is essentially different from the case with non-vanishing observed events.

The tests, q_μ and \tilde{q}_μ , are then

$$\begin{aligned}
q_\mu &= -2 \ln \frac{\mathcal{L}(\mu, \hat{\theta}_1(\mu), \hat{\alpha}_k(\mu), \dots)}{\mathcal{L}(\hat{\mu}, \hat{\theta}_1, \hat{\alpha}_1, \dots)} \\
&= 2(\mu - \hat{\mu}) \sum_{i=1}^{N_{\text{bins}}} s_i (1 + \sum_{k=1}^{N_{\text{sys}}} \delta_i^k \bar{\alpha}_k) - (\mu^2 - \hat{\mu}^2) \sum_{k=1}^{N_{\text{sys}}} \left(\sum_{i=1}^{N_{\text{bins}}} s_i \delta_i^k \right)^2, \tag{B11}
\end{aligned}$$

$$\begin{aligned}
\tilde{q}_\mu &= -2 \ln \frac{\mathcal{L}(\mu, \hat{\theta}_1(\mu), \hat{\alpha}_k(\mu), \dots)}{\mathcal{L}(0, \hat{\theta}_1(0), \hat{\alpha}_1(0), \dots)} \\
&= 2\mu \sum_{i=1}^{N_{\text{bins}}} s_i (1 + \sum_{k=1}^{N_{\text{sys}}} \delta_i^k \bar{\alpha}_k) - \mu^2 \sum_{k=1}^{N_{\text{sys}}} \left(\sum_{i=1}^{N_{\text{bins}}} s_i \delta_i^k \right)^2. \tag{B12}
\end{aligned}$$

We can see that the effect of background systematic uncertainties is vanishing for \tilde{q}_μ and its effect on q_μ is via $\hat{\mu}$ and also greatly reduced because of a single bin with the least background-to-signal ratio in Eq. B8. It means that the distribution of the tests is mainly due to signal systematic uncertainties.

Assuming all signal systematic uncertainties are small, we neglect the last term in Eq. B11 and treat the auxiliary data $\bar{\alpha}_{ks}$ as independent random variables abiding by a normal distribution. The standard derivation of q_μ , denoted as Δq_μ , would be approximately

$$\frac{\Delta q_\mu}{q_\mu} = \sqrt{\sum_{k=1}^{N_{\text{sys}}} \left(\frac{\sum_{i=1}^{N_{\text{bins}}} s_i \delta_i^k}{\sum_{i=1}^{N_{\text{bins}}} s_i} \right)^2}, \tag{B13}$$

We can see that only the yield-related uncertainties matter here (otherwise $\sum_{i=1}^{N_{\text{bins}}} s_i \delta_i^k = 0$). If all uncertainties affect the yield only, we have (writing δ_i^k as δ^k)

$$\frac{\Delta q_\mu}{q_\mu} = \sqrt{\sum_{k=1}^{N_{\text{sys}}} (\delta^k)^2}, \tag{B14}$$

We can see that it is equal to κ in Eq. A11. Therefore, in the case of no observed events, we assume that the standard derivation of the tests is due to signal related systematic uncertainties only and

$$\frac{\Delta q_\mu}{q_\mu} = \frac{\Delta \tilde{q}_\mu}{\tilde{q}_\mu} = \kappa, \tag{B15}$$

where κ is defined in Eq. 31.

Taking the Ex. 0 in Sec. IV as example, Fig. 22 shows the distribution of \tilde{q}_μ in the case of 0 events in the toy experiments as well as the prediction in this work. We have also checked

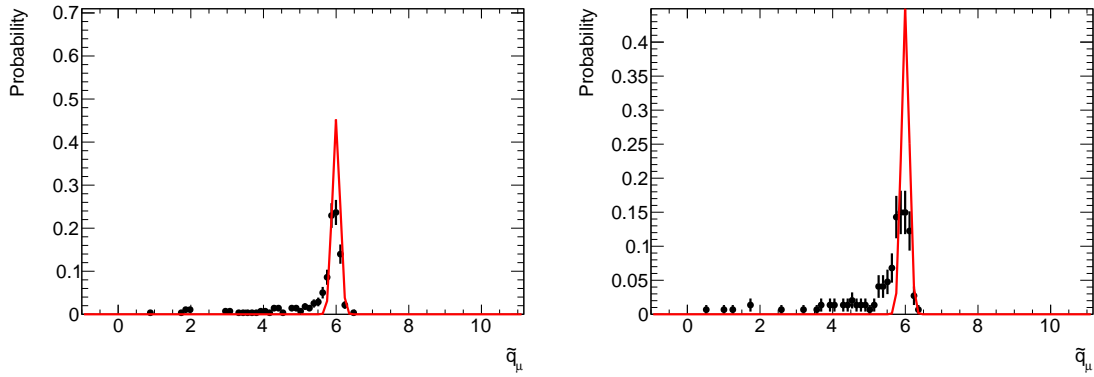


FIG. 22. The distribution of \tilde{q}_μ in Ex. 0 from the toy experiments under the hypothesis $\mu_H = 0$ (Left) and $\mu_H = \mu = 3$ (Right). The red curve represents the prediction in this work.

several real measurements and found that the assumption above is reasonable. It should be noted that the same conclusion holds if there are bins with 0 expected signal events because of their little contribution to measuring the signal strength. In the 6-bin model, the last bin has the least signal-to-background ratio and a negligible signal expectation. Therefore, in Eq. 36 we adopt the following $\sigma(\hat{\mu})$ if $k_0 = k_1 = k_2 = k_3 = k_4 = 0$, to make the assumption in Eq. B15 hold.

$$\sigma(\hat{\mu}) = \begin{cases} \kappa \frac{\mu - 2\hat{\mu}}{2}, & \text{for } \tilde{q}_\mu \\ \kappa \frac{\mu - \hat{\mu}}{2}, & \text{for } q_\mu \end{cases} \quad (\text{B16})$$

As shown above, the optimal value, $\hat{\mu}$, is at its lowest bound, $\sim -b_0/s_0$, in the case of observing 0 events. But this is not the only case. For $\hat{\mu}$ at the lowest bound, the basic difference is that the first-order derivative of the logarithmic likelihood function is non-vanishing and will contribute to the likelihood-ratio tests. The binned model in current work does not include any nuisance parameter or freely-floating parameter and cannot predict the spread of the test statistic's distribution well. Therefore, in such cases, we propose to use the following $\sigma(\hat{\mu})$.

$$\sigma(\hat{\mu}) = \sqrt{\sigma_0^2 + (\kappa\hat{\mu})^2 + (\kappa \frac{\mu - c\hat{\mu}}{2})^2} \quad (\text{B17})$$

Here $c = 1$ for q_μ and $c = 2$ for \tilde{q}_μ . This is just the combination of the uncertainty in the

usual case in Eq. 29 and that in the 0-event case in Eq. B16.

- [1] ATLAS Collaboration, Phys. Lett. B 716 (2012) 1, arXiv:1207.7214.
- [2] CMS Collaboration, Phys. Lett. B 716 (2012) 30, arXiv:1207.7235.
- [3] G. Cowan, K. Cranmer, E. Gross, and O. Vitells, Eur. Phys. J. C 71 (2011) 1554, Eur. Phys. J. C 73 (2013) 2501 (Erratum), arXiv:1007.1727
- [4] A. Wald, *Tests of Statistical Hypothesis Concerning Several Parameters When the Number of Observations is Large*, Transactions of the American Mathematical Society, Vol. **54**, No. 3, pp. 426-482.
- [5] L.-G. Xia, JHEP **08** (2021) 071, arXiv:2012.15618, version 1.
- [6] G. Cowan, Statistical Data Analysis, Clarendon Press, Oxford, 1998.
- [7] L.-G. Xia, J. Phys. **G 46** (2019) 085004, arXiv:1805.03961.
- [8] S. Algeri, J. Aalbers, K. D. Morå, and J. Conrad, Nature Rev.Phys. 2 (2020) 5, 245-252, arXiv: 1911.10237.
- [9] ATLAS Collaboration, JHEP 07 (2023) 088, arXiv: 2207.00348
- [10] G. Zech, Nucl. Instrum. Meth. **A 277** (1989) 608.
- [11] A. L. Read, J. Phys. **G 28** (2002) 2693.